Aus dem Institut für Zahn-, Mund- und Kieferheilkunde
der Medizinischen Fakultät Charité – Universitätsmedizin Berlin

DISSERTATION

The structural integrity of post-and-core (root canal) restorations: a 3D high-resolution in vitro study

Die strukturelle Integrität von Stiftaufbau Restaurationen (Wurzelstift): eine hochauflösende 3D-In-vitro-Studie

zur Erlangung des akademischen Grades
Doctor of Philosophy (PhD)

vorgelegt der Medizinischen Fakultät
Charité – Universitätsmedizin Berlin

von

Ana Prates Soares

Datum der Promotion: 26.06.2022

Table of Contents

List of Figures

1. Abstract in English and German

1.1. Abstract

Introduction: After a root-canal treatment many teeth need to be restored employing post-and-core restorations. The final restoration presents an assortment of biomaterials that must function as a unity to withstand chewing loading in a wet environment. Post-and-core restorations occasionally fail, and their structure usually exhibits voids, air bubbles, or delamination. However, the evaluation of the structural integrity and the attachment between components of post-and-core restorations is a challenge.

Objective: To develop and apply a non-destructive methodology to evaluate the presence of defects in post-and-core restorations using x-ray synchrotron imaging techniques. It was hypothesized that the selected techniques would be able to non-destructively detect flaws in the structure of post-and-core restorations.

Materials and methods: Human root canal treated upper incisors (n=14) were restored with post-and-core build-ups using prefabricated fiberglass (Dentin Post, Komet) or titanium posts (Kopfstift Titanium Post, Komet), cemented with a self-adhesive resin cement (RelyX Unicem 2, 3M ESPE Dental Products), sustaining cores made with a flowable resin composite (Rebilda DC Quickmix, Voco) that were adhered to the tooth substrate and posts by a universal adhesive system (Futurabond U, Voco). Synchrotron x-ray sources were used for dental sample imaging with phase contrast-enhanced micro-CT (PCE-CT), while single fiberglass posts were imaged with PCE-CT and synchrotron x-ray refraction radiography (SXRR). The reconstructed volumes were segmented, and the data were analysed manually (by a single operator) and digitally in 2D and 3D. The generated data were tabulated and used for statistical analysis.

Results: The resulting images from PCE-CT of post-and-core restored teeth revealed the presence of gaps between tooth and cement in ~45% of the interface in the cervical area of the restoration. Endodontic epoxy-based sealer was found in ~10% of the interface. No gaps between post and cement were observed, as well as no statistical difference between fiberglass and titanium post groups for all measured parameters. PCE-CT was suitable to reveal gaps between the adhesive system from the core and the tooth substrate. The segmented gaps were non-uniformly distributed and occupied on average ~34% of the interface and were

between 2 and 16 µm thick. PCE-CT and SXRR revealed the impact of bur trimming of fiberglass posts for canal fitting. The regions affected by trimming showed a strong accumulation of defects like splinters, cracks, and fragments of glass fibres extending from the bur-touched surface to 50 µm deep in the post structure.

Conclusion: The cutting-edge non-destructive imaging technology used in the present work is invaluable for revealing the defects in post-and-core restorations. The identified defects are possible causes of treatment failure. Further work is needed to show the progressive effect of defects under load over time.

1.2. Zusammenfassung

Einleitung: Nach einer Wurzelkanalbehandlung müssen Zähne regelmäßig mittels eines Wurzelaufbaus wiederhergestellt werden. Die endgültige Restaurierung erfordert den Einsatz verschiedener Biomaterialien, die als Einheit fungieren müssen, um der Kaubelastung in feuchter Umgebung standzuhalten. Stift-Stumpf-Aufbauten versagen gelegentlich und ihre Struktur weist häufig Hohlräume, Luftblasen oder Delaminationen auf. Die Bewertung der strukturellen Festigkeit und der Verbindung zwischen den einzelnen Komponenten der Stift-Stumpf-Aufbauten sowie der Auswirkung etwaiger vorhandener Defekte ist jedoch schwierig.

Ziel: Entwicklung und Anwendung einer zerstörungsfreien Methode zur Bewertung des Vorhandenseins von Defekten in Stift-Stumpf-Aufbauten mithilfe von Röntgensynchrotron-Bildgebungstechniken. Es wurde die Hypothese aufgestellt, dass die ausgewählten Techniken in der Lage sind, Defekte in der Struktur von Stift-Stumpf-Aufbauten zerstörungsfrei zu erkennen.

Material und Methoden: Menschliche wurzelkanalbehandelte obere Schneidezähne (n = 14) wurden mit Stift-Stumpf-Aufbauten unter Verwendung von vorgefertigten Glasfaser (Dentin Post, Komet) oder Titanstiften (Kopfstift Titanium Post, Komet) restauriert, die mit einem selbstadhäsivem Befestigungskompositen zementiert wurden (RelyX Unicem 2, 3M ESPE Dental Products). Stumpf-Aufbauten aus einem fließfähigen Aufbaukomposit (Rebilda DC Quickmix, Voco) wurden mit einem universellen Adhäsivsystem (Futurabond U, Voco) auf das Zahnsubstrat und die Stifte geklebt. Synchrotron-Röntgenquellen wurden für die Bildgebung von Zahnproben mit phasenkontrastverstärkter Mikro-CT (PCE-CT) verwendet. Einzelne Glasfaserstifte wurden mit PCE-CT und Synchrotron-Röntgenrefraktionsradiographie (SXRR) abgebildet.Die rekonstruierten Volumina wurden segmentiert und die Daten manuell (von einem einzelnen Bediener) und digital in 2D und 3D analysiert. Die generierten Daten wurden tabellarisch dargestellt und für statistische Analysen verwendet.

Ergebnisse: Die mithilfe der PCE-CT erstellten Bilder der Stift-Stumpf-Aufbauten zeigten in ~45% Lücken in der Verbindung zwischen Zahn und Zement im zervikalen Bereich der Restauration. Endodontische epoxidharzbasierte Sealer wurde in ~10% der Grenzflächen gefunden. Es wurden keine Lücken zwischen Stift und Zement sowie keine kein statistische Unterschiede zwischen Glasfaser- und Titanstiftgruppen für alle gemessenen Parameter

beobachtet. Mittels PCE-CT wurden die Lücken zwischen dem Adhäsivsystem des Stumpfs und dem Zahnsubstrat sichtbar. Die segmentierten Lücken waren ungleichmäßig verteilt, zwischen 2 und 16 µm groß und fanden sich durchschnittlich auf rund 34% der Oberflächen. PCE-CT und SXRR zeigten die Auswirkungen des Bohrertrimmens der Glasfaserstifte für die Kanalanpassung. Die vom Trimmen betroffenen Bereiche zeigten eine starke Ansammlung von Defekten wie Splittern, Rissen und Glasfaser--Fragmenten, nicht nur an der vom Bohrer berührten Oberfläche, sondern bis zu 50 µm tief in der Stiftstruktur.

Fazit: Die in der vorliegenden Arbeit verwendete hochmoderne zerstörungsfreie Bildgebungstechnologie ist von unschätzbarem Wert, um Defekte in Stift-Stumpf-Aufbauten aufzudecken. Die identifizierten Defekte sind mögliche Ursachen für ein Versagen der Behandlung. Weitere Arbeiten sind erforderlich, um den fortschreitenden Effekt eines Defekts unter Belastung im Laufe der Zeit aufzuzeigen.

2. Current scientific knowledge

2.1. Rehabilitation of root canal treated teeth using post-and-core restorations:

Dental post-and-core build-ups are regularly used for restoring teeth with severely compromised dental structure (Guldener et al., 2017). Built into the root canal and former pulp chamber, the post-and-core restoration is composed of a central pillar cemented to the canal walls and covered by a restorative material. The post sustains a bulk of material that replaces the lost dental substance, the entire construct will support an artificial crown, designed to rehabilitate the function and aesthetics of the damaged tooth (Fig. 1). Contrary to what was once believed (Saupe et al., 1996), the post does not reinforce the remaining root walls, rather, it retains the core and artificial crown (Madfa et al., 2014). Ultimately, the post-and-core restoration should sustain recurring chewing loads in the oral cavity acting as a single unit (monoblock), which requires that the different components attach firmly to each other (Tay & Pashley, 2007). However, the evaluation of the structural integrity and the attachment between components of post-and-core restorations is a challenge, as well as the investigation of the effect of the presence of defects in the restoration.

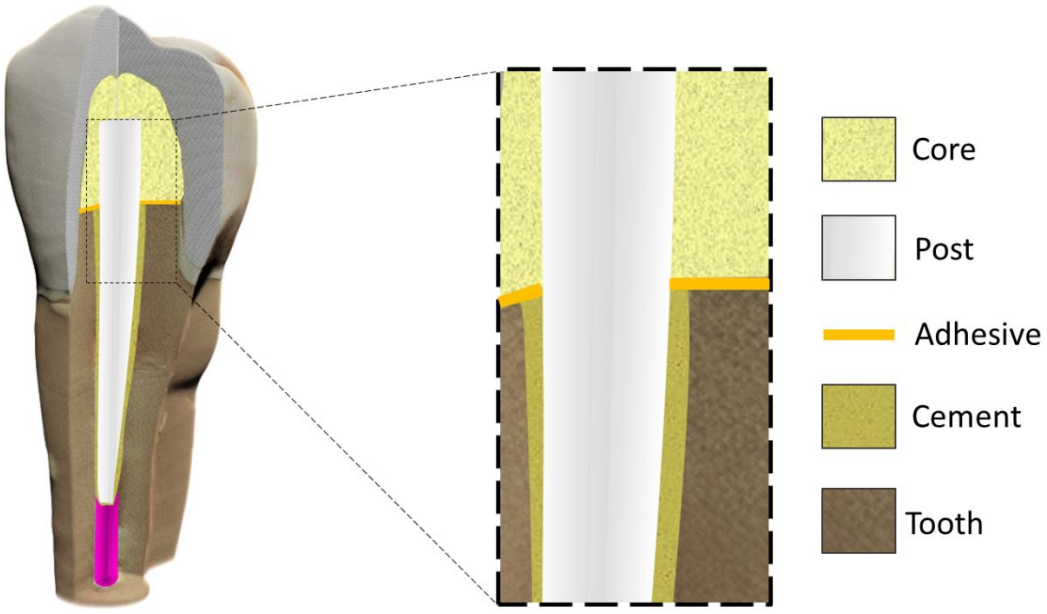

Figure 1: 3D rendering of a root canal-filled tooth rehabilitated with a ceramic crown sustained by a post-and-core restoration. Core build-up composite material; Post; Adhesive used to bond core and tooth substrate; Cement that attaches the post to the root canal walls; Tooth substrate. *Figure created by the author, based on her data.*

Due to developments in manufacturing techniques, cementation methods, and reduced costs of modern composite biomaterials, a range of products are now available for clinical use in post-and-core restorations.

Nowadays, there are two main types of clinically used posts: custom-made and prefabricated posts (Samran et al., 2013). Custom-made posts are cast using different metallic alloys (Gold, Nickel-Chrome, etc.) or they are made individually of non-metallic materials (Zirconia, Fiberglass, etc.). Prefabricated posts are more common and can either be metallic or non-metallic, with different surface designs (Fig. 2). The main advantage of prefabricated posts is that the restoration of the root canal-treated tooth takes place in one short clinical procedure. Currently, the most popular posts in clinical use are prefabricated fibre posts (Ahmed et al., 2017), and from those, fiberglass posts are the most frequently used (Naumann et al., 2016). They have a major advantage in that they provide better aesthetics (Bateman et al., 2003) and present a similar elastic modulus to the tooth's (Duret et al., 1996) as compared with titanium and other metallic prefabricated posts.

Figure 2: examples of clinically used prefabricated posts. In sequence from left to right: GT® Fibre Post (Dentsply), ParaPost®XH (Coltene Whaledent), ParaPost®Taper Lux (Coltene Whaledent), CosmoPost® (Ivoclar Vivadent), E-Post (Injecta), CF Carbon Fibre Post (J Morita), Golden Plated Screw Post (Rogin). *Figure created by the author, based on pictures of different post devices.*

Posts are cemented in the root canal, using one of many commercially available dedicated materials. Types of cement that self-adhere to root dentin or those that cure in dual mode (chemically and by light activation), such as self-adhesive resin cement and resin-modified glass ionomer cement, are typically selected by the dentist due to their easiness of use (Ahmed et al., 2017).

While using prefabricated posts, there are different options for direct core build-up materials. The ideal material must have a similar-to-teeth mechanical response to withstand chewing

loads, as well as have tooth-like colour for aesthetic reasons (Kumar & Shivrayan 2015; Panitiwat & Salimee, 2017). Various dental resin composites exist that are well able to adhere to both tooth and post through a bonding system (Panitiwat & Salimee, 2017). Specifically, resin composites are used by most clinicians as routine core build-up materials in Germany (Naumann et al., 2016).

Adhesive systems are responsible for attaching dental biomaterials to the tooth substrate. The use of adhesive in dentistry dates back to 1955 (Buonocore, 1955), and currently, there is an abundance of products in the market (Van Meerbeek et al., 2003). The latest generation of bonding systems is known as universal adhesives and was developed for easiness of use, with two application modes, one requiring acid etching of the tooth substrate and one that does not (Sofan et al., 2017).

2.2. Failures of post-and-core restorations:

It is an unfortunate reality that post-and-core restorations occasionally fail, often together with the crowns built on them (Marchionatti et al, 2017). There are several reasons why post-and-core restorations may fail. One group of causes includes biological factors, such as pathogens penetrating through the root and crown restorations leading to reinfection of the root canal system and secondary caries (Naumann et al., 2017). Further mechanical/structural factors, such as restoration cracking may lead to restoration detachment and loss or entire tooth fracture (Naumann et al., 2017). Both biological and mechanical factors may lead to the loss of the treated tooth. The impact of tooth loss on the quality of life of treated individuals ranges from imposing social/aesthetic discomfort to speech impairment (Okoje et al., 2012). There is, therefore, an ever-increasing pressure to conservatively and reproducibly restore teeth following root canal therapy. This is driven forward by the increase in the general knowledge of patients regarding desirable dental treatments and a higher demand for effectiveness and longevity of restorations (Douglass & Sheets, 2000). The first prospective study reporting a 10-year follow-up of fiberglass post restorations showed a 4.6% annual failure rate (Naumann et al., 2012). The results show that almost 50% of the posts failed within ten years following placement. A later prospective multi-centre study with a patient follow-up of 6.5 years reported an 8.6% annual failure rate of teeth restored with post-and-core (Kramer et al., 2019). A more recent retrospective study showed a mean survival of 12 years for post-and-core restored teeth (Martino et al., 2020). Although dental treatment is never

considered "everlasting", annual failure rates as listed above are sub-standard and may badly impact tooth survival.

2.3. Possible causes for post-and-core restoration failure:

While the failure of restorations may come about for many reasons, ranging from biological contamination to trauma, there exists a specific group of failures that relate to structural failures due to inadequacy of the artificially restored tooth. Such failures ensue following the appearance and growth of structural defects. In post-and-core restorations, failures may occur due to detachment of the structures (adhesive failures) or due to fractures of the constructed restorations (cohesive failures). To better understand, predict and prevent structural defects, there is a need to evaluate the materials currently used in post-and-core restorations, at high resolution and under conditions that are closest to the in-operative conditions in the oral cavity. Such data is essential to improve fabrication/construction methods and better select the ideal materials.

2.4. Investigation of flaws in post-and-core restorations:

The extent to which failures in post-and-core restorations occur due to flaws in the materials remains unknown (Rasimick et al., 2010). Though often failures are attributed to mistakes during clinical procedures, it is important to note that even if the restorative process follows treatment protocols meticulously, the final restoration that combines different interfaces and different materials (Fig. 1) often ends up containing voids, air bubbles, or delamination (Lorenzoni et al., 2013). Especially the interface between tooth tissue (dentin, in the roots), cement, and post is of major concern as it forms the ‘weak link’ (Teshigawara et al., 2019). Flaws in the restoration are considered to be damaging to its integrity and presumably worsen prognosis (Da Silva et al., 2015), as they concentrate stress during mechanical load, which may lead to cracking and detachment under cyclic chewing loads. Thus, it is essential to identify the relationship between structural defects and restoration.

Assessing the internal structure of post-and-core restorations is a challenge. Morphological studies of the root canals containing post-and-core restorations are conventionally performed by mapping out serial cross-sections of the sample’s contours with different microscopes (Heintze, 2013). While useful, this method is essentially destructive and can introduce damage (eg. cracks) during sample preparation (Zaslansky et al., 2011). Furthermore, cross-sections of

the samples only expose 2D surfaces of the 3D dental structure, and sample slicing leaves no possibility for later mechanical testing, which may be necessary to quantify the effects of such defect. Therefore, there is a need to examine post-and-core restorations using more reproducible and non-destructive techniques such as computer tomography (CT) methods (Grande et al., 2012). However, due to the small dimensions and the complex material structuring, internal non-destructive tomographic examination of dental post-and-core restorations is extremely challenging. X-ray micro-computed tomography (micro-CT) is an imaging modality of increasing importance that uses x-ray projections and allows reconstruction of 3D (virtual) models of the tooth interior in a non-destructive manner with spatial resolutions in the micron scale. Most CT techniques use absorption (attenuation) contrast as a proxy for mapping the atomic density of the elements that constitute the material (Gao et al., 2006). Materials with similar absorption coefficients or those with low absorption are not well imaged by this technique (Betz et al., 2007) because the signal-to-noise ratios and the resulting contrast are too low as compared with background noise (Chen et al., 2010). Since many of the materials used in the dense mm-sized teeth for restorative proposes have similarly low densities, separating them using absorption contrast in micro-CT is often unfeasible (Rominu et al., 2014).

Phase contrast-enhanced micro-computed-tomography (PCE-CT), which exploits phase shifts in the x-ray beam as it propagates through the structure (Gao et al., 2006; Baruchel et al., 2001), relies on small differences in the scattering properties of materials and interfaces, providing high contrast images at sub-micron spatial resolutions (Betz et al., 2007). PCE-CT requires high-power x-ray sources and is therefore performed in large-scale research facilities known as 'synchrotrons'. Imaging beamlines in such facilities comprise large laboratories with high flux, high brilliance x-ray. With laser-like (partial coherence) configurations, such imaging setups deliver micro-CT imaging capacities at sub-micrometre resolutions (Anderson et al., 2014). Data acquired with PCE-CT in synchrotron radiation facilities have provided more accurate information of the presence and extent of voids and spaces in root canal treated teeth than laboratory micro-CT (Zaslansky et al., 2011). Further, the x-ray can be used for other non-destructive measurement techniques that can be applied for the examination of dental composites. For instance, x-ray refraction is a radiographic technique that can image large fields of view (several mm) and can detect nanoscale size defects in composites (Müller et al., 2018).

3. Research objective

The present work investigates flaws in the structure of post-and-core restorations at interfaces and within materials commonly used in the clinic for rehabilitating severely compromised teeth following root canal treatment. It was hypothesized that the selected high-resolution, x-ray synchrotron imaging techniques would be able to non-destructively detect flaws in the structure of post-and-core restorations.

The **main objective** was to develop and use a non-destructive methodology to evaluate the presence of defects in post-and-core restorations employing x-ray synchrotron imaging techniques. To do so, phase contrast-enhanced micro-computed tomography (PCE-CT) and synchrotron x-ray refraction radiography (SXRR) were used and the acquired data were evaluated qualitatively and quantitatively through image analysis. A **second objective** was to understand the prevalence and probability of occurrence of micro-gaps within chairside restored post-and-core restorations. For that, different components of the restoration were assessed for their characteristics: cement, post-and-core build-up. A **third objective** was to evaluate the attachment between the different biomaterials as well as to the tooth substrate. To carry it out, the attachment between tooth and cement, cement and post, core bonding system and tooth, as well as core build-up material and post, were estimated.

Three papers were produced, each generating different outputs to accomplish the objectives:

- Paper 1: the non-destructive assessment of attachment at the interfaces between post, cement, and root canal wall, as well as the characteristics of the cement that might correlate to the prevalence of interfacial gaps using PCE-CT.

- Paper 2: the establishment of a non-destructive methodology to quantify interfacial gaps between adhesive system and tooth substrate using PCE-CT.

- Paper 3: the establishment of a new methodology to assess fiberglass post structure as well as the evaluation of the effect of post trimming for canal fitting using PCE-CT and SXRR.

4. Methodology

4.1. Overview

A summary of the methodology is surveyed in the next paragraphs. Details of each material and method referenced in the text can be found in the methodology sections of the three publications that form the core of my thesis.

4.2. Sample preparation

As detailed in Paper 1, human upper central incisors were obtained under an ethics-approved protocol (EA4/102/14) by the Ethical Review Committee of the Charité Universitätsmedizin Berlin. The teeth were measured, selected, and prepared following a strict protocol, described in paper 1. The restorative steps were systematically followed in each of the 14 samples in a standardized clinically relevant manner performed by one single operator. All the samples were kept wet throughout the treatment and in all imaging experiments to simulate clinical humid conditions. An illustration of the steps can be seen in Fig. 3.

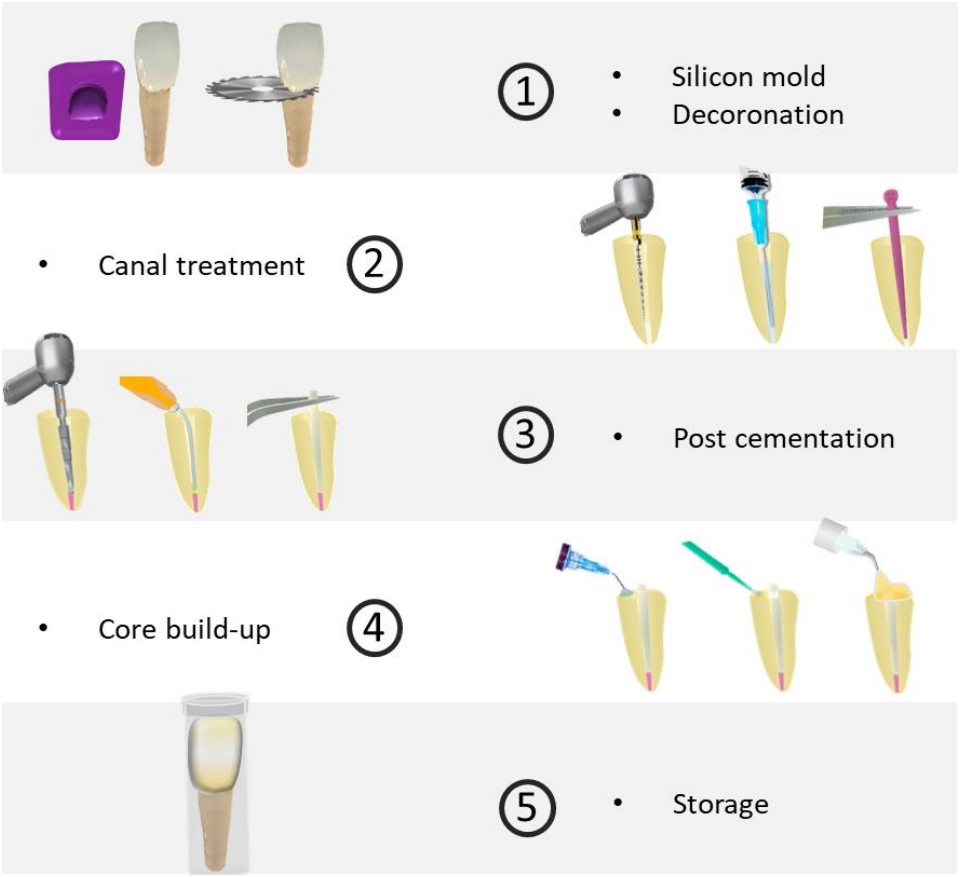

Figure 3: General depiction of the steps taken to produce samples for the current work. 1. An impression of the crown of each sample was made using a silicon putty before decoronation with a diamond-band saw. 2. Each root canal was treated following a strict protocol of instrumentation, irrigation, and finally canal obturation. 3.

Part of the obturated canal was drilled to receive a post, which was cemented with a self-adhesive composite. 4. The core and overall anatomy of the crown were restored using a core build-up composite attached to the etched and bonded cervical tooth substrate. 5. The final step was to trim and fit the samples into individual plastic vials padded with wet foam to keep them humid. *Figure created by the author, based on her data.*

4.3. Laboratory micro Computer Tomography (micro-CT)

A laboratory micro-CT scanner (Skyscan 1172; Bruker micro CT, Kontich, Belgium) was used to obtain radiographic projections of each sample according to the steps detailed in papers 1, 2, and 3 (Fig. 4). The images were acquired using pixel sizes between 2~14 µm at 50~100 kV with 0.2~0.5° rotational angle steps around (360°) the longitudinal axis of the samples (1000~4000 ms exposure times). The volumes were then reconstructed using the micro-CT manufacturer's own software and algorithm (NRecon 1.7.1.0, Bruker micro-CT, Kontich, Belgium).

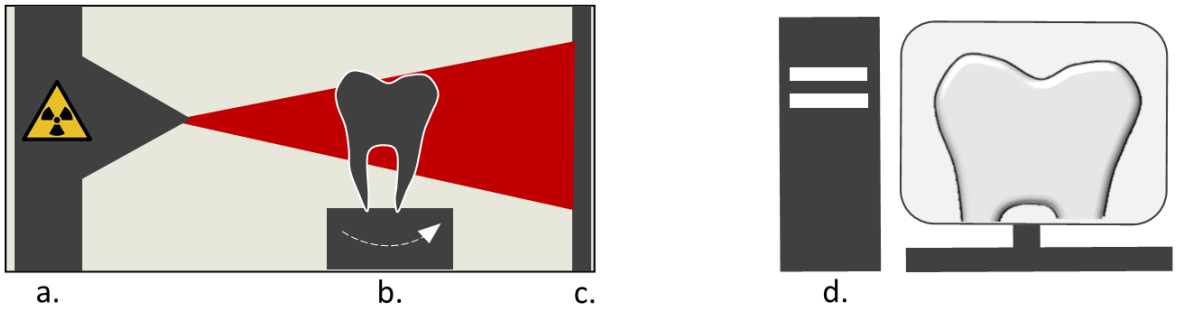

Figure 4: Illustration of Laboratory micro-CT scanner, the sample is placed inside the micro-CT equipment on a rotation stage (b). A cone-shaped x-ray beam is generated (a) and used to take sequential radiographies from different angles of the specimen acquired by an x-ray camera (c). The acquired radiographies are then used for a virtual reconstruct of the tooth structure in 3D (d). *Figure created by the author, based on her data.*

4.4. Use of synchrotron x-ray source for sample imaging

Synchrotrons are large-scale research facilities mainly used for generating x-rays (Fig. 5). At the heart of these machines, electrons are produced with a linear accelerator and deflected by magnetic fields to first accelerate through a booster ring to then be stored while traveling at very high speeds in a second ring (main ring). Every time the electrons are deflected by magnets that steer the electrons inside the vacuum ring, x-rays are generated. Synchrotron x-ray beams have very high flux and a high coherence that can be utilized in the experimental end station hutches of the beamlines. Different beamlines are optimized for different imaging techniques and/ or specific applications. Most often beamlines are composed of three main hutches: the first is the optics, where x-ray mirrors and crystals enable the selection energy

used in different experiments; the second is the experimental hutch, where the sample is placed and the interaction with the x-ray beam is detected; the third hutch is used for control or auxiliary experiments, e.g. it is where imaging settings are defined and the quality of the acquired data is verified.

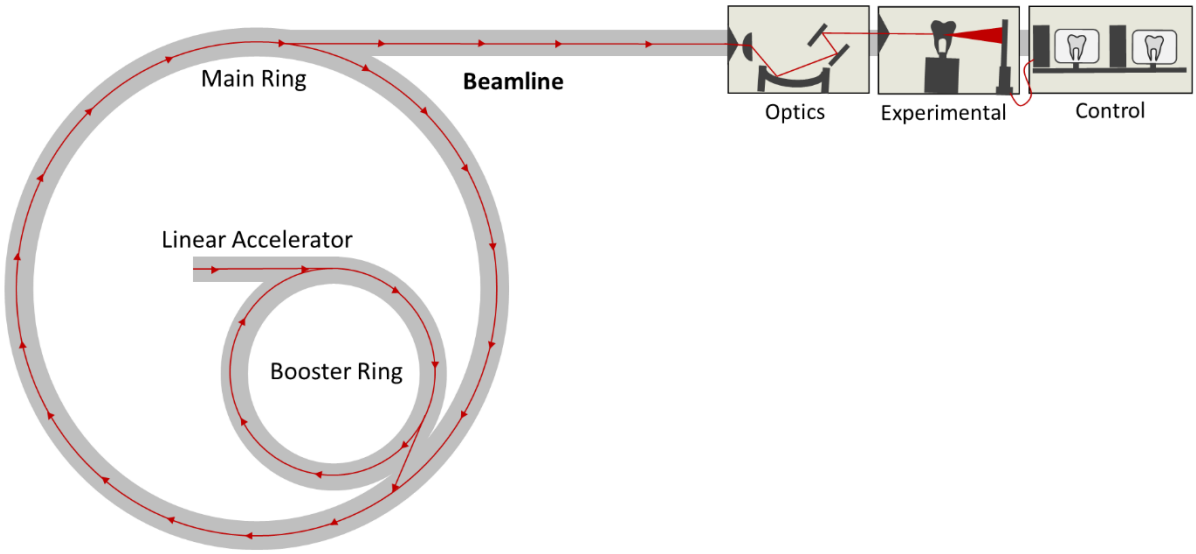

Figure 5: Schematic representation of a synchrotron facility showing the different parts of its structure: the Linear Accelerator, where the electrons are generated; both of the rings Booster and Main, where the electrons are stored and constantly deflected by magnetic fields to generate high brilliance x-ray light; and an exemplary beamline with its optics, experimental and control hutches. *Figure created by the author, based on her data.*

Two different synchrotron Beamlines were used in the present work: ID19 at the European Synchrotron Radiation Facility (ESRF, Grenoble, France) for papers 1 and 2, and BAMline at the Berliner Elektronenspeicherring-Gesellschaft für Synchrotronstrahlung (Bessy, Helmholtz Zentrum Berlin, Berlin, Germany) for paper 3 (Fig. 6).

4.4.1. Synchrotron-based Phase contrast-enhanced micro-CT (PCE-CT):

In phase contrast-enhanced micro-CT (PCE-CT) radiographs with enhanced contrast at edges are generated by changes in the wave propagation of the x-ray beam (Baruchel et al., 2001). It relies on the subtle differences between densities of the materials comprising the structures and leads to better contrast in the projections so that finer details in density fluctuations can be observed (Betz et al., 2007). For PCE-CT, propagation phase-contrast enhancement is achieved by an increased distance between sample and detector leading to significant edge enhancement, an intensification of the contrast at the edges of the imaged features (Fig. 6) (Cloetens et al., 1996). Phase-contrast imaging increases the contrast by about two orders of

magnitude as compared to attenuation-based methods (Lewis, 2004). The use of a parallel beam allowed imaging at sub-micron pixel sizes (0.64 – 0.876 µm). In synchrotron beamlines, high-resolution images are acquired using high-end large detectors with high speed and high magnification capabilities. PCE-CT was used in all papers 1, 2, and 3.

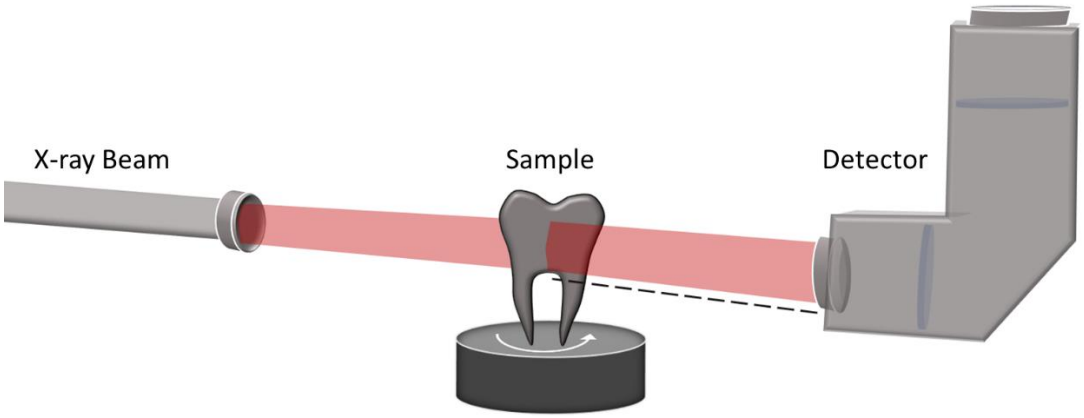

Figure 6: Schematic illustration of an imaging experiment using phase contrast-enhanced micro-CT (PCE-CT), the x-ray beam reaches the experimental hutch with the selected wavelength and energy. The sample placed on a rotation stage is imaged in different angles by a highly sensitive detector. Importantly, an increased distance is needed between the sample and detector (discontinued line) to induce edge enhancement (Cloetens et al., 1996). *Figure created by the author, based on her data.*

4.4.1.1. Image Processing and Reconstruction

PCE-CT data reconstruction occurs in several steps and includes pre-processing/filtering (normalization), contrast adjustment (phase-retrieval), and 3D reconstruction (Fig. 7) before quantification and/or visualization (2D slices and 3D renderings). In the pre-processing step, the raw radiographies or projections acquired during the experiment are normalized. To do so, multiple images of the x-ray beam on (flat fields) and off (dark field) are used. Flat fields unify the intensities across the images and eliminate noise due to the variations in the beam flux, intensity fluctuations, presence of streaks and speckles in the imaging system. And dark fields are used to remove noise generated by the detector electronics. Contrast-adjustment by phase processing yields contrast enhanced radiographs filtered employing phase retrieval using Paganin-based filtering (δ/β ratio of 200, Mirone et al., 2014). In the reconstruction step, full volumes were reconstructed by the back-projection method (Nrecon 1.7.1.0, Bruker micro-CT or Octopus v. 8.5 (Vlassenbroeck et al., 2007) for Bessy data, and PyHST for ESRF data). A horizontal stitching mode was specifically used for samples wider than the detector field of view.

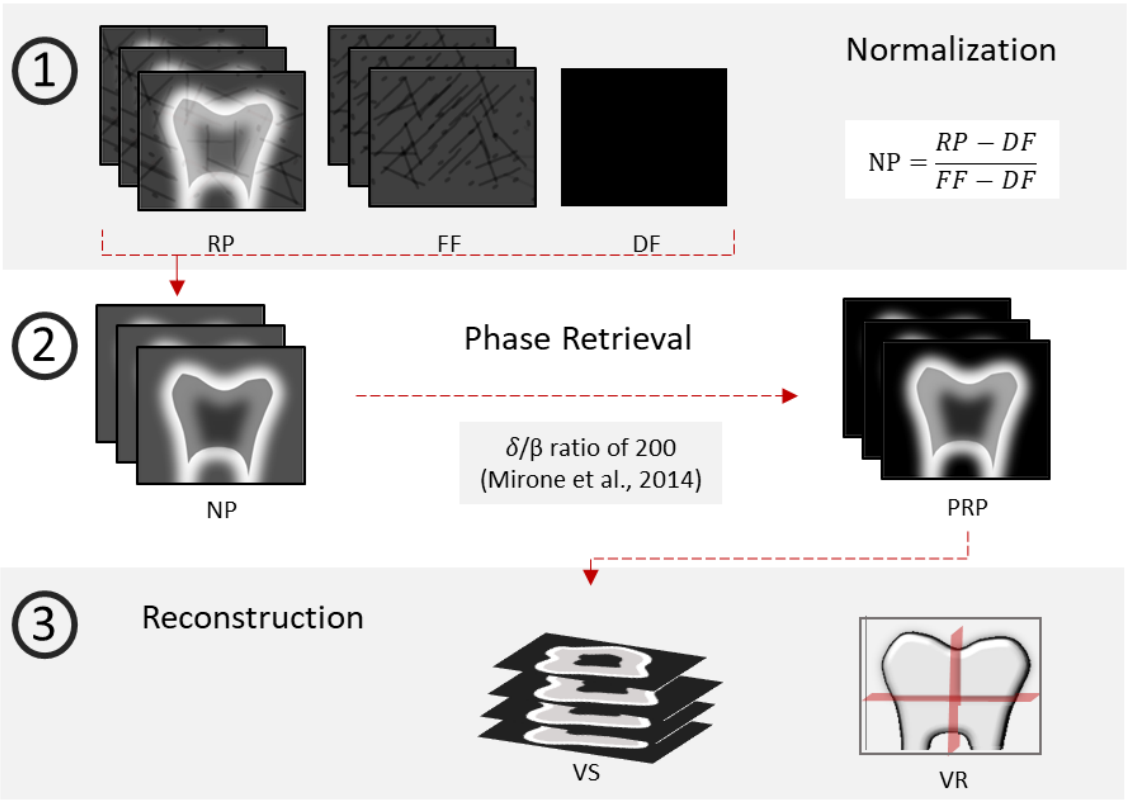

Figure 7: Illustration of steps required for image processing 1. Normalization of the Raw Projections (RP) acquired with PCE-CT was done by subtracting the Dark Filed Projection (DF) and dividing by the Flat Fields Projections (FF). 2. Phase retrieval was performed on the Normalized Projections (NP) using the Paganin-based filtering (δ/β =200; Mirone et al., 2004) generating Phase Retrieved Projections (PRP) with higher contrast. 3. Reconstruction of the volumes were performed using a back-projection method to generate Virtual Slices (VS) and Volume Renderings (VR) of the imaged samples. *Figure created by the author, based on her data.*

4.4.1.2. Image Analysis and Segmentations

The reconstructed volumes consisted of grayscale images rich with information about the interaction of different materials and tooth substrate. Each gray value present in the volumes corresponded to a different component in the sample (biomaterial or dental tissue). The different gray values could all be visualized in a histogram, which also showed the frequency of their appearance in the images. Sample components that were more prevalent in the volume showed up as higher peaks in the histogram, while less prevalent components with more gray variation are portrayed as wider and shorter peaks. The different components can then be separated or segmented from the volumes by cropping the desired areas of the histogram, also known as thresholding (Fig. 8).

Different computer softwares were used to visualize and segment the volumes in the present work. In paper 1, manual measurements were performed using ImageJ (ImageJ 1.52d,

National Institutes of Health, Rockville, USA) and renderings with CTvox (Bruker micro-CT, Kontich, Belgium) as explained in the Materials and Methods of the paper. In papers 2 and 3, different components in the volumes were segmented by value (histogram cropping/threshold) and shape using ImageJ and Amira (AmiraZIBEdition version 2020.48, Zuse Institute Berlin (ZIB), Germany, and Thermo Fisher Scientific, Bordeaux, France).

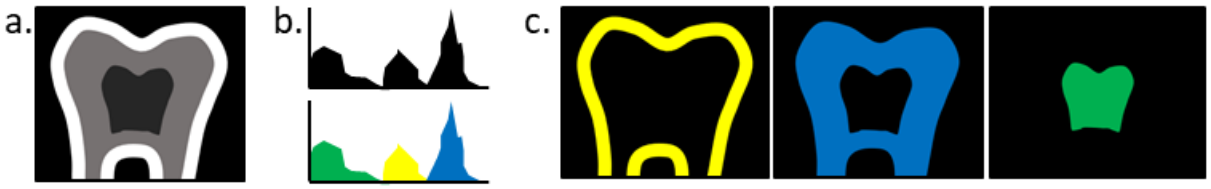

Figure 8: Schematic representation of image segmentation. 3D reconstructed data volumes from PCE-CT are composed of grayscale images (a). The gray values can be compiled and visualized in the form of a histogram (b). The different gray values represent different components of the original image and can be segmented by threshold (c) of the histogram (histogram cropping).

4.4.2. Synchrotron X-Ray Refraction Radiography (SXRR)

Single fiberglass posts were imaged by synchrotron-based x-ray refraction radiography (SXRR) in a synchrotron facility (BAMline at Helmholtz-Zentrum Berlin, Germany). A schematic of the experiment is shown in Fig 9. As detailed in paper 3 of the present thesis, the SXRR uses the ability of an analyser crystal (b, Fig. 9) to angularly separate the x-rays refracted at different interfaces. It is placed between sample (a, Fig. 9) and detector (c, Fig. 9). The analyser crystal only discriminates refracted x-rays within its scattering plane (blue plane, Fig. 9), thus the SXRR resulting images depend on the orientation of the inner surfaces of the fiberglass post. Once the fiberglass posts were positioned vertically, meaning, with its fibres parallel to the scattering plane (∥, a & d, Fig. 9), only flaws and cracks that might appear perpendicular to the post longitude could be revealed. While when the fiberglass post was positioned perpendicularly (⊥, a & d, Fig. 9) to the scattering plane, the flaws that were longitudinal or appeared in between fibres could be revealed.

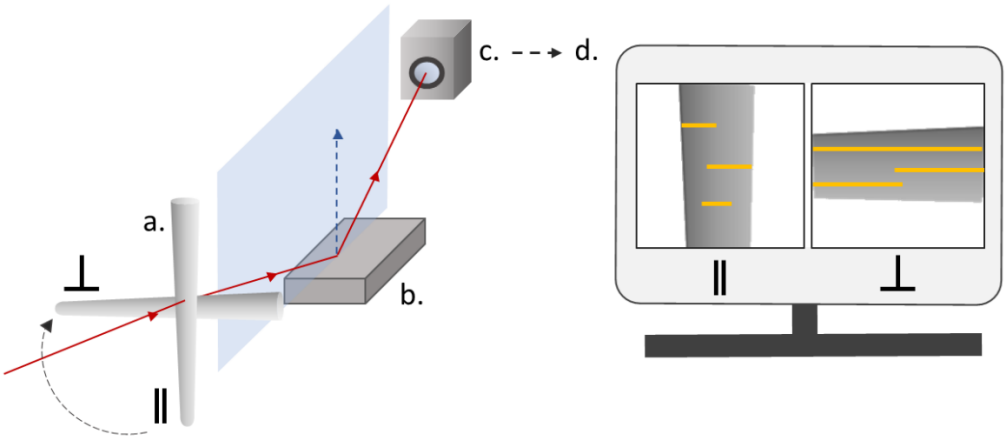

Figure 9: Schematic image of synchrotron-based x-ray Refraction Radiography (SXRR) imaging (red arrow line = x-ray beam) of fiberglass posts (a) the samples were positioned first parallel (‖) and then perpendicular (⊥) to the scattering plane (blue plane) and scattering vector (blue arrow) of the analyser crystal (b). The images were acquired by a detector (c), and depicted flaws (d, yellow lines) perpendicular to the fiberglass long axis (‖, when the sample was parallel to the scattering plane) or longitudinal flaws (⊥, when the samples were perpendicular to the scattering plane). *Figure created by the author, based on her data.*

4.5. Scanning Electron Microscopy (SEM)

Scanning electron microscopy (SEM) was used in paper 1 for the supporting information section. Samples were cross-sectioned and dried to be imaged with the SEM (Phenom XL, Thermo Fisher Scientific, Massachusetts, USA) as described in the supporting information. Images acquired with SEM were used to validate the capacity of PCE-CT to reveal all the components and flaws present in the sample's structure.

4.6. Statistical Analysis

Statistical comparison between different parameters in two independent groups on papers 1 & 3 was tested using either a parametric (t-test) or a non-parametric test (Mann-Whitney) depending on the data's normal distribution. In paper 1, a 2-way ANOVA test with a t-test (LSD) post hoc test was also used for the statistical comparison of 4 independent groups with normally distributed data. Pearson correlation test was used in paper 1 to test the linear correlation between different variables. The significance level was $p<0.05$ for all the tests.

5. Main results

5.1. Overview

This work focused on revealing and assessing flaws in the structure of post-and-core restorations. Complementary aspects of the restorations were investigated generating 3 papers. In paper 1, post cementation inside the root canal was imaged and assessed. In paper 2, a novel method was established for imaging and measuring gaps in bonding sites of the core build-up to the tooth structure. Finally, in paper 3 fiberglass posts structures were assessed for damage with or without diamond bur trimming. The results for each paper are briefly summarized in the following paragraphs. Further details and figures are presented in the published papers attached.

5.2. Results from Paper 1

In paper 1, we were able to successfully assess the attachment at the interfaces between post, cement, and root canal wall in post-and-core restorations prepared with a self-adhesive resin cement (RelyX Unicem 2) and two different types of posts: fiberglass and titanium. Furthermore, we were able to assess factors that correlated to the prevalence of interfacial gaps.

The laboratory micro-CT generated volumes provided the overall geometry of the samples, which were then used for planning of the high-resolution experiment using PCE-CT (example in Fig. 10, for more detailed figures, see paper 1, Fig. 1 & 2). High tooth density and low attenuation from the self-adhesive resin cement limited the visualization of the root canal restorations when imaged with laboratory micro-CT. The cervical first millimetre of the canal was imaged using PCE-CT, which produced high-quality images validated by SEM micrographs as shown in paper 1, Supporting Information, Figure S1.

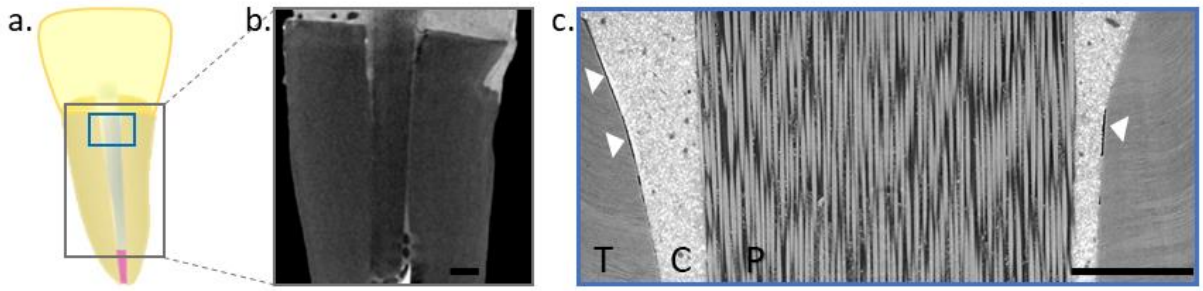

Figure 10: representation of the resulting images from Paper1. The samples (a) were imaged with Laboratory micro-CT (b), and the resulting volumes were used for examining the overall geometry of the post-and-core restoration. The specific cervical 1st mm of the canal was selected for imaging with PCE-CT (c), which revealed interfacial gaps between tooth and cement (white arrowheads). Tooth (T), Cement (C), Fiberglass Post (P). Scale bar: 500 µm. *Figure created by the author, based on her data.*

PCE-CT volumes revealed multiple components within the sample: root canal dentin, self-adhesive resin cement, fiberglass and titanium posts, and remnants of root canal sealer (an epoxy resin-based sealer, AH Plus, Dentsply Sirona, Ballaigues, Switzerland) - used for canal obturation. Flaws in the restoration were also revealed: pores, gaps, and delamination. The morphology of the restorations was examined in virtual cross-sectional slices along the sample long axis at every 100 µm. All the measured parameters averages and standard deviations are shown in paper 1, Supporting information, Table S1. Canal perimeter, canal area, post perimeter, post area, cement layer area, gap perimeter, sealer covered perimeter are tabulated by the depth and divided into two groups.

Due to the canal taper and the post structure, the amount of cement in the canal decreased by depth as shown in the graph in paper 1, Fig. 3b. There was a steady amount of interfacial gaps between root canal wall and self-adhesive resin cement of ~45% along the canal (paper 1, Fig. 3c); while there was a persistent amount of canal sealer remnant at the same interface of ~10% along the canal (paper 1, Fig. 3d). There were no interfacial gaps between post and cement, and no statistically significant difference between all measured variables in fiberglass and titanium posts restorations (paper 1, Supporting information, Table S1). The presence of sealer remnants, the cement area, as well as the perimeter and area of the canal were moderately correlated to the prevalence of interfacial gaps (Pearson correlation test, $r = 0.52 \sim 0.55$, $p < 0.001$, in paper 1 Supporting information, Table S1).

5.3. Results from Paper 2

In paper 2, we effectively established a methodology to quantify interfacial gaps between a universal adhesive system (tested on the bonding system Futurabond U) and tooth substrate, and the morphology and distribution of the gaps could be evaluated in detail without sample slicing.

Laboratory micro-CT scans were used to identify and select the area of the adhesive system used for core build-up bonding to the tooth cervical area (paper 2, Fig. 5). In Laboratory micro-CT scans the adhesive showed as empty spaces beneath the core, due to its low absorption coefficient. The settings and post-processing steps established in paper 2 to acquire the PCE-CT volumes from post-and-core restorations were effective in revealing not only the adhesive layer but also gaps at the interface between tooth and adhesive (paper 2, Fig 2-7). The use of PCE-CT also clearly revealed the micromorphology of the dentin tubules as well as their spatial distribution.

The amount, extension, and thickness of the interfacial gaps between adhesive and dentin were able to be measured non-destructively, as high-quality with high-resolution volumes from PCE-CT were segmented through threshold and label selection (further details in paper 2, Image analysis section). In the examined samples, interfacial gaps occupied on average 34% (±15%) of the interface and were between 2 and 16 µm thick. The gaps were non-uniformly distributed at the interface and some sides of the sample's core seemed almost completely detached from the tooth (paper 2, Figure 7).

5.4. Results from Paper 3

In paper 3, we were able to establish a new methodology to examine the micromorphology and integrity of fiberglass posts, especially the integrity of single fibers in the post. Furthermore, we successfully assessed the effect of diamond bur trimming on the post structure.

SXRR provided 2D images (radiographies) that revealed the flaws in fiberglass at a nanoscale resolution (at least x10 < 4 µm). While the posts were perpendicular (⊥) to the scattering plane of the analyser crystal, the interfacial gaps between glass fibres and the composite matrix were shown as highly prevalent (bright lines) throughout the structure of the post (paper 3, Fig. 2). Scans of posts parallel (∥) to the scattering plane, showed that there are no

flaws across the structure of the post. The regions affected by diamond bur trimming showed a strong accumulation of defects visible in both parallel and perpendicular imaging, not only at the bur-touched surface but up to 50 µm deep in the post (red arrowheads, paper 3, Fig. 2).

PCE-CT 3D volumes revealed the 3-dimensional structure of the posts at ~1 µm resolution. Glass fibres, composite matrix, filler particles (oxides used to make the post structure more radiopaque for medical radiographies), and voids were shown in the volumes as well as their spatial distribution (paper 3, Fig. 3). The bur trimmed areas of the posts exhibited cracked fibres, glass fragments, and splinters still embedded up to 50 µm deep in the composite matrix. The high-quality volumes could be segmented and analysed using two different techniques: in 2D and 3D as described in Appendix A and B of paper 3, respectively. The results of the 2D analysis (paper 3, Table 1) showed the significant effect of bur-trimming on the fibres area, perimeter, thickness, circularity, and roundness ($p < 0.001$), meaning that the bur-affected areas had substantial changes in the size and shape of the fibres. While the 3D analysis (paper 3, Table 2) results display the effect of bur-trimming on the 3D thickness and volume of the fibres ($p < 0.001$). The spatial distributions of the glass fibres within the composite matrix were not significantly altered in the bur affected regions as verified in 2D by the Voronoi analysis and in 3D by the Voronoi fibre distance (paper 3, Tables 1 & 2). Furthermore, most fibres affected or not by trimming were slightly curved, measured by the degree of tortuosity (paper 3, Table 2).

PCE-CT could not reveal the same interfacial gaps between glass fibres and composite matrix as SXRR, due to their difference in resolution and sensitivity. However, both techniques were complementary to each other in assessing the bur-trimmed area, while SXRR can clearly identify the spot and extent, PCE-CT can reveal the morphological effects of bur-trimming on fiberglass posts.

6. Clinical implications and open research questions

6.1. Clinical implications

Post-and-core treatments are widely used for the restoration of endodontically treated teeth with a large loss of crown substrate. The long-term prognosis of post-and-core restorations is limited, and prospective studies have shown a mean annual failure of up to 8.6% (Kramer et al., 2019). Many factors can impact the prognosis of a post-and-core treatment, such as the type of tooth restored, the presence of a ferrule (Naumann et al., 2012) age and sex of the patient, proximal contacts (Kramer et al., 2019), among others. While clinical studies can detect the result of the treatment failure, they can only speculate about the underlying mechanism. Isolating each factor in vivo is a great challenge, thus there is a need for thorough in vitro testing. Therefore, identifying flaws in post-and-core restorations is important for understanding possible causes of treatment failure and ultimately for fomenting improvements in clinical protocols to achieve a better treatment prognosis.

Cutting edge non-destructive imaging technology used in the present work, such as micro-CT, phase contrast-enhanced imaging, and refraction radiography now provides us the means to investigate post-and-core restorations with a level of detail that other techniques do not achieve. Specifically, it is now possible to reveal non-destructively the presence of micro gaps within a biomaterial structure or between the different restorative components. In my work, I established different methodologies for quantification of flaws in cement, bonding system, and fiberglass post, as well as discontinuities at their interfaces in a moist root canal, treated tooth.

A uniform attachment between all restorative components and tooth substrate is considered essential to establish a stable structure, also called a monoblock (Tay & Pashley, 2007). The results of this work were published in three articles in internationally renowned journals. The results of all three publications show the difficulties in achieving a desirable sound structure with continuous bonding between biomaterials in post-and-core restorations. For example, it is clear from the data from paper 3, that trimming fiberglass posts is highly destructive to its structure. In papers 1 and 2, the bonding between the tooth substrate and the cement or bonding system, respectively, is highly inhomogeneous. Gaps at the interfaces may function as stress raisers that under chewing forces may increase in size, spreading throughout the interface which may ultimately lead to restorative failure. Further work is needed to analyse

the progressive effect of defects (presence of interfacial gaps) over time when the tooth is put into function.

The materials selected for the present work are broadly used in current clinical practice. Dental materials are evaluated by biological and mechanical tests following the International Organization for Standardization (ISO) standards. However, the results in the present thesis revealed a significant accumulation of flaws in post-and-core restorations. The data presented here make the case for additional testing to dental materials. The present methodology can in the future be applied to examine new materials before their employment in inpatient care.

6.2. Open research questions

The insights generated in these projects open interesting new paths that could foster improvement in diagnosing post-and-core failures and the development of new materials.

6.2.1. Diagnosis of post-and-core restoration failure

Synchrotron x-rays cannot be used clinically. However, loss restorations or loss teeth from patients that received restorative post-and-core treatment can in the future be examined in high-resolution using the presently described methodology. The 3D non-destructive examination can generate further data about the type of failure and if one or more features are more prominent in teeth loss cases. Another way to correlate tooth loss to restorative flaws would be imaging in vitro samples before and after cyclic loading using the present methodology. Then, it would be possible to see where cracks can initiate in the restoration structure, and how they relate to flaws within and at the interface of the different materials.

6.2.2. Development of accurate in silico testing

With the information assembled in the present project, more accurate computer simulation models can be created in the future for testing the interaction between materials and tooth substrate in silico. Computer models that depict morphological features and the real flawed interaction between biomaterial and tissue could generate more precise computer calculations. Slight changes in different parameters in the model and mechanical simulations could be applied to isolate different factors and test their influence on the overall prognosis of the restoration. Future developments could completely replace in vitro testing of tooth restoration by virtual simulations without loss of predictive value.

6.3. Conclusion

There is sufficient evidence to support the claim that the selected imaging techniques can non-destructively detect flaws in the structure of post-and-core restorations. The cutting-edge imaging technology used in the present work is invaluable for revealing the defects in post-and-core restorations. Moreover, the identified flaws are possible causes of treatment failure. Further work is needed to analyse the progressive effect of defect under load over time, to correlate flaws with clinical findings and treatment survival, and to develop more accurate in silico models for material testing.

7. Bibliography:

1. Ahmed S.N., Donovan T.E., Ghuman T. Survey of dentists to determine contemporary use of endodontic posts. *J Prosthet Dent.* **117**, 642-645 (2017).

2. Anderson P.J., Yong R., Surman T.L., Rajion Z.A., Ranjitkar S. Application of three-dimensional computed tomography in craniofacial clinical practice and research. *Aust Dent J.* **59**, 174-85 (2014).

3. Baruchel J., Lodini A., Romanzetti S., Rustichelli F., Scrivani A. Phase-contrast imaging of thin biomaterials. *Biomaterials.* **22**, 1515-20 (2001).

4. Bateman G, Ricketts DN, Saunders WP Fibre-based post systems: a review. *Br Dent J.* **195**, 43-8 (2003).

5. Betz O., Wegst U., Weide D., Heethoff M., Helfen L., Lee W.K., Cloetens P. Imaging applications of synchrotron x-ray phase-contrast microtomography in biological morphology and biomaterials science. I. General aspects of the technique and its advantages in the analysis of millimetre-sized arthropod structure. *J Microsc.* **227**, 51-71 (2007).

6. Buonocore M.G. A simple method of increasing the adhesion of acrylic filling materials to enamel surfaces. *J Dent Res*. **34**, 849-53 (1955).

7. Chen G.H., Zambelli J., Bevins N., Qi Z., Li K. X-ray phase sensitive imaging methods: basic physical principles and potential medical applications. *Curr Med Imaging Rev.* **6**, 90-99 (2010).

8. Cloetens P., Barrett R., Baruchel J., Guigay J.-P., Schlenker M. Phase objects in synchrotron radiation hard x-ray imaging. *J. Phys. D Appl. Phys.* **29**, 133–146 (1996).

9. Da Silva N.R., Aguiar G.C., Rodrigues M.de P., Bicalho A.A., Soares P.B., Veríssimo C., Soares C.J. Effect of resin cement porosity on retention of glass-fiber posts to root dentin: an experimental and finite element analysis. *Braz Dent J.* **26**, 630-6 (2015).

10. Douglass C.W., Sheets C.G. Patients' expectations for oral health care in the 21st century. *JADA* **131**, s3-7 (2000).

11. Duret B., Duret F., Reynaud M. Long-life physical property preservation and post endodontic rehabilitation with the Composipost. *Compend Contin Educ Dent Suppl.* **20**, S50-6 (1996).

12. Gao X., Luo S., Yin H., Liu B., Xu M., Yuan Q., Gao X., Zhu P. A micro-tomography method based on x-ray diffraction enhanced imaging for the visualization of micro-organs and soft tissues. *Comput Med Imaging Graph.* **30**, 339-47 (2006).

13. Grande N.M., Plotino G., Gambarini G., Testarelli L., D'Ambrosio F., Pecci R., Bedini R. Present and future in the use of micro-CT scanner 3D analysis for the study of dental and root canal morphology. *Ann Ist Super Sanita.* **48**, 26-34 (2012).

14. Guldener K.A., Lanzrein C.L., Siegrist Guldener B.E., Lang N.P., Ramseier C.A., Salvi G.E. Long-term Clinical Outcomes of Endodontically Treated Teeth Restored with or without Fiber Post-retained Single-unit Restorations. *J Endod.* **43**, 188-193 (2017).

15. Heintze S.D. Clinical relevance of tests on bond strength, microleakage and marginal adaptation. *Dent Mater.* **29**, 59-84 (2013).

16. Kramer E.J., Meyer-Lueckel H., Wolf T.G., Schwendicke F., Naumann M., Wierichs R.J. Success and survival of post-restorations: six-year results of a prospective observational practice-based clinical study. *Int Endod J.* **52**, 569-578 (2019).

17. Kumar G., Shivrayan A. Comparative study of mechanical properties of direct core build-up materials. *Contemp Clin Dent.* **6**, 16-20 (2015).

18. Lewis R.A. Medical phase contrast x-ray imaging: current status and future prospects. *Phys Med Biol.* **49**, 3573-83 (2004).

19. Lorenzoni F.C., Bonfante E.A., Bonfante G., Martins L.M., Witek L., Silva N.R. MicroCT analysis of a retrieved root restored with a bonded fiber-reinforced composite dowel: a pilot study. *J Prosthodont.* **22**, 478-83 (2013).

20. Madfa A.A., Kadir M.R., Kashani J., Saidin S., Sulaiman E., Marhazlinda J., Rahbari R., Abdullah B.J., Abdullah H., Abu Kasim N.H. Stress distributions in maxillary central incisors restored with various types of post materials and designs. *Med Eng Phys.* **36**, 962-7 (2014).

21. Marchionatti A.M.E., Wandscher V.F., Rippe M.P., Kaizer O.B., Valandro L.F. Clinical performance and failure modes of pulpless teeth restored with posts: a systematic review. *Braz Oral Res.* **3**, 31:e64. (2017).

22. Martino N., Truong C., Clark A.E., O'Neill E., Hsu S.M., Neal D., Esquivel-Upshaw J.F. Retrospective analysis of survival rates of post-and-cores in a dental school setting. *J Prosthet Dent.* **123**, 434-441 (2020).

23. Mirone A., Brun E., Gouillart E., Tafforeau P., Kieffer J. The PyHST2 hybrid distributed code for high speed tomographic reconstruction with iterative reconstruction and a priori knowledge capabilities. *Nucl. Instrum. Methods Phys. Res. B* **324**, 41–48 (2014).

24. Müller B.R., Cooper R.C., Lange A., Kupsch A., Wheeler M., Hentschel M.P., Staude A., Pandey A., Shyam A., Bruno G. Stress-induced microcrack density evolution in β-eucryptite ceramics: Experimental observations and possible route to strain hardening. *Acta Materialia* **144**, 627-641 (2018).

25. Naumann M., Koelpin M., Beuer F., Meyer-Lueckel H. 10-year survival evaluation for glass-fiber-supported postendodontic restoration: a prospective observational clinical study. *J Endod.* **38**, 432-5 (2012).

26. Naumann M., Neuhaus K.W., Kölpin M., Seemann R. Why, when, and how general practitioners restore endodontically treated teeth: a representative survey in Germany. *Clin Oral Investig.* **20**, 253-9 (2016).

27. Naumann M., Sterzenbach G., Dietrich T., Bitter K., Frankenberger R., von Stein-Lausnitz M. Dentin-like versus Rigid Endodontic Post: 11-year Randomized Controlled Pilot Trial on No-wall to 2-wall Defects. *J Endod.* **43**, 1770-1775 (2017).

28. Okoje V.N., Dosumu O.O., Alonge T.O., Onyeaso C. Tooth loss: are the patients prepared? *Niger J Clin Pract.* **15**, 172-5 (2012).

29. Panitiwat P., Salimee P. Effect of different composite core materials on fracture resistance of endodontically treated teeth restored with FRC posts. *J Appl Oral Sci.* **25**, 203-210 (2017).

30. Rasimick B.J., Wan J., Musikant B.L., Deutsch A.S. A review of failure modes in teeth restored with adhesively luted endodontic dowels. *J Prosthodont.* **19**, 639-46 (2010).

31. Rominu M., Manescu A., Sinescu C., Negrutiu M.L., Topala F., Rominu R.O., Bradu A., Jackson D.A., Giuliani A., Podoleanu A.G. Zirconia enriched dental adhesive: a solution for OCT contrast enhancement. Demonstrative study by synchrotron radiation microtomography. *Dent Mater.* **30**, 417-23 (2014).

32. Samran A., El Bahra S., Kern M. The influence of substance loss and ferrule height on the fracture resistance of endodontically treated premolars. An in vitro study. *Dent Mater.* **29**, 1280-6 (2013).

33. Saupe W.A., Gluskin A.H., Radke R.A. Jr. A comparative study of fracture resistance between morphologic dowel and cores and a resin-reinforced dowel system in the intraradicular restoration of structurally compromised roots. *Quintessence Int.* **27**, 483-91 (1996).

34. Schwartz R.S., Robbins J.W. Post placement and restoration of endodontically treated teeth: a literature review. *J Endod.* **30**, 289-301 (2004).

35. Sofan E., Sofan A., Palaia G., Tenore G., Romeo U., Migliau G. Classification review of dental adhesive systems: from the IV generation to the universal type. *Ann Stomatol (Roma)* **8**, 1-17 (2017).

36. Tay F.R., Pashley D.H. Monoblocks in Root Canals: A Hypothetical or a Tangible Goal. *J Endod.* **33**, 391-8 (2007).

37. Teshigawara D., Ino T., Otsuka H., Isogai T., Fujisawa M. Influence of elastic modulus mismatch between dentin and post-and-core on sequential bonding failure. *J Prosthodont Res.* **63**, 227-231 (2019).

38. Van Meerbeek B., De Munck J., Yoshida Y., Inoue S., Vargas M., Vijay P., Van Landuyt K., Lambrechts P. and Vanherle G. Buonocore memorial lecture. Adhesion to enamel and dentin: Current status and future challenges. *Operative Dentistry* **28**, 215-235 (2003).

39. Vlassenbroeck J., Dierick M., Masschaele B., Cnudde V., Hoorebeke L., Jacobs P. Software tools for quantification of x-ray microtomography. *Nucl Instrum Methods Phys Res A* **580**, 442–5 (2007).

40. Zaslansky P., Fratzl P., Rack A., Wu M.K., Wesselink P.R., Shemesh H. Identification of root filling interfaces by microscopy and tomography methods. *Int Endod J.* **44**, 395-401 (2011).

8. Declaration of your own contribution to top-journal publications for a PhD

I, Ana Prates Soares (APS) was a main contributor to all aspects of the below listed publications:

Paper 1: Soares AP, Bitter K, Lagrange A, Rack A, Shemesh H, Zaslansky P. **Gaps at the interface between dentine and self-adhesive resin cement in post-endodontic restorations quantified in 3D by phase contrast-enhanced micro-CT**. International Endodontic Journal. 2020.

Contribution:
Literature research: I performed a thorough review of literature on the topic and created the outline of the paper with the guidance of Paul Zaslansky and Hagay Shemesh.

Sample collection: The samples were collected and selected by me with the guidance of Kerstin Bitter and Paul Zaslansky.

Sample preparation: I set the protocols of sample preparation and prepared the samples in the laboratory with the guidance of Kerstin Bitter and Hagay Shemesh.

Experiments:

- **Laboratory micro-CT**: I scanned the samples and reconstructed the volumes with the guidance of Paul Zaslansky.
- **Synchrotron phase-contrast enhanced micro-CT**: I scanned the samples following the protocols and guidance of Paul Zaslansky and Alexander Rack.
    - **Image processing**: I processed the images and reconstructed the volumes with the assistance of Adrien Lagrange and the guidance of Paul Zaslansky and Alexander Rack.
- **Image analysis**: I set up the methodology of image analysis and performed it with guidance of Paul Zaslansky.
- **Data analysis**: I compiled, tabulated, and analysed the data with the guidance of Kerstin Bitter, Hagay Shemesh and Paul Zaslansky. I performed the statistical analysis.

Production of Figures: I produced all the images.

Supporting information: the section was produced by me with guidance of Paul Zaslansky including the performance of:

- **Scanning electron microscopy**: the samples were sliced, dried, and imaged by me with a Scanning electron microscope.
- **Figures**: all figures conception and design were performed by me.
- **Graphics**: the graphics were made by me after data analysis.
- **Table**: the table was made by me after statistical analysis of the data.

Preparation of Manuscript: I wrote the manuscript, which was revised by all other authors. The paper was finalized and set to publication by me and Paul Zaslansky. The corrections suggested during peer-review phase were performed by me and Paul Zaslansky.

Paper 2: Soares AP, Blunck U, Bitter K, Paris S, Rack A, Zaslansky P. **Hard X-ray phase-contrast-enhanced micro-CT for quantifying interfaces within brittle dense root-filling-restored human teeth**. Journal of Synchrotron Radiation. 2020.

Contribution:

Literature research: I performed a thorough review of literature on the topic and created the outline of the paper with the guidance of Paul Zaslansky and Uwe Blunck.

Sample collection: I collected and selected the samples with the guidance of Kerstin Bitter and Paul Zaslansky.

Sample preparation: The protocols of sample preparation were set by me with the guidance of Kerstin Bitter, Sebastian Paris and Uwe Blunck. I prepared all the samples in the laboratory.

Experiments:

- **Laboratory micro-CT**: I scanned the samples and reconstructed the volumes.
- **Synchrotron phase-contrast enhanced micro-CT**: The samples were scanned by me following the protocols and guidance of Paul Zaslansky and Alexander Rack.
    - **Image processing**: The images were processed, and the volumes were reconstructed by me with the guidance of Paul Zaslansky and Alexander Rack.
- **Image analysis**: The methodology of image analysis was setup and performed by me.
- **Volume segmentation**: I segmented all the volumes.
- **Thickness analysis**: The analysis of the Interfacial Gap thickness was performed by me with guidance from Paul Zaslansky.
- **Data analysis**: The data was analysed by me with intellectual input from Kerstin Bitter, Uwe Blunck, Sebastian Paris and Paul Zaslansky.

Production of Figures: I produced all the figures and tables with the guidance of Paul Zaslansky and Alexander Rack.

Preparation of Manuscript: I wrote the manuscript which was reviewed by all co-authors. The paper was finalized and set to publication by me. The corrections suggested during peer-review phase were performed by me and Paul Zaslasnky.

Paper 3: Soares AP, Baum D, Hesse B, Kupsch A, Müller BR., Zaslansky P. **Scattering and phase-contrast X-ray methods reveal damage to glass fibers in endodontic posts following dental bur trimming**. Dental Materials. 2020.

Contribution:

Literature research: I performed a thorough review of literature on the topic and created the outline of the paper with the guidance of Paul Zaslansky and Bernhard Hesse.

Sample collection: The samples were collected and selected by me and trimmed by Paul Zaslansky.

Experiments:

- **Synchrotron x-ray refraction radiography**: the measurements were performed by Bernd Müller and Andreas Kupsch. The images were then sent to me. The analysis and interpretation of the radiographies was done by me with guidance from Bernd Müller, Andreas Kupsch and Paul Zaslansky.
- **Synchrotron phase-contrast enhanced micro-CT**: I scanned the samples following the protocols and guidance of Paul Zaslansky.
    - **Image processing**: I processed the images and reconstructed the volumes.
- **Image segmentation**: I performed image segmentation in 2D with guidance from Bernhard Hesse. Image segmentation in 3D was done by me and Daniel Baum.
- **Image analysis**: The resulting images from SXRR and the segmented volumes from PCE-CT were interpreted and analysed by me with guidance from Daniel Baum, Bernhard Hesse and Paul Zaslansky.
- **Data analysis**: I compiled, tabulated and analysed the data with the guidance of Daniel Baum. Statistical analysis of the data was performed by me.

Production of Figures: I produced all the figures and tables with the guidance of Paul Zaslansky, Daniel Baum and Bernd Müller.

Supporting information: the section was produced by me with guidance of Paul Zaslansky including the performance of:

- **Sample preparation**: the samples were prepared by me.
- **Scanning electron microscopy**: the samples were scanned by Paul Zaslansky and the figures were produced by me.
- **Radiography from synchrotron x-ray Refraction Radiography**: the linear attenuation image was generated by measurements made by Bernd Müller and Andreas Kupsch.
- **PCE-CT reconstruction analysis in 2D and 3D**: the images and methods were designed and made by me with guidance from Paul Zaslansky, Bernhard Hesse and Daniel Baum.
- **Laboratory micro-CT samples imaging and analysis**: the samples were scanned and analysed by me with guidance from Paul Zaslansky.

Preparation of Manuscript: I wrote the manuscript which was reviewed by all the co-authors. I finalized the paper and set it to publication. The corrections suggested during peer-review phase were performed by me and Paul Zaslansky.

_____

Signature, date and stamp of first supervising university professor / lecturer

_____

Signature of doctoral candidate

9. Statutory Declaration

"I, Ana Prates Soares, by personally signing this document in lieu of an oath, hereby affirm that I prepared the submitted dissertation on the topic "**The structural integrity of post-and-core (root canal) restorations: a 3D high-resolution in vitro study**" "**Die strukturelle Integrität von Stiftaufbau Restaurationen (Wurzelstift): eine hochauflösende 3D-In-vitro-Studie**", independently and without the support of third parties, and that I used no other sources and aids than those stated.

All parts which are based on the publications or presentations of other authors, either in letter or in spirit, are specified as such in accordance with the citing guidelines. The sections on methodology (in particular regarding practical work, laboratory regulations, statistical processing) and results (in particular regarding figures, charts and tables) are exclusively my responsibility.

Furthermore, I declare that I have correctly marked all of the data, the analyses, and the conclusions generated from data obtained in collaboration with other persons, and that I have correctly marked my own contribution and the contributions of other persons (cf. declaration of contribution). I have correctly marked all texts or parts of texts that were generated in collaboration with other persons.

My contributions to any publications to this dissertation correspond to those stated in the below joint declaration made together with the supervisor. All publications created within the scope of the dissertation comply with the guidelines of the ICMJE (International Committee of Medical Journal Editors; www.icmje.org) on authorship. In addition, I declare that I shall comply with the regulations of Charité – Universitätsmedizin Berlin on ensuring good scientific practice.

I declare that I have not yet submitted this dissertation in identical or similar form to another Faculty.

The significance of this statutory declaration and the consequences of a false statutory declaration under criminal law (Sections 156, 161 of the German Criminal Code) are known to me."

Date Signature

10. Journal Summary List for Paper 1

Paper 1: Soares AP, Bitter K, Lagrange A, Rack A, Shemesh H, Zaslansky P. Gaps at the interface between dentine and self-adhesive resin cement in post-endodontic restorations quantified in 3D by phase contrast-enhanced micro-CT. *Int Endod J*. 2020 Mar;53(3):392-402.

Excerpt of the InCites Journal Citation Report in Web of Science™ by Clarivate Analytics

Journal Data Filtered By: **Selected JCR Year: 2019**, as there is no list yet for 2020.
Selected Editions: SCIE, SSCI Selected Categories: '**DENTISTRY, ORAL SURGERY & MEDICINE**'
Selected Category Scheme: WoS
In total: 91 Journals

Rank	Full Journal Title	Total Cites	Journal Impact Factor	Eigenfactor Score
1	PERIODONTOLOGY 2000	5,159	7.718	0.006380
2	JOURNAL OF CLINICAL PERIODONTOLOGY	14,785	5.241	0.013050
3	JOURNAL OF DENTAL RESEARCH	20,557	4.914	0.019900
4	DENTAL MATERIALS	15,316	4.495	0.013480
5	ORAL ONCOLOGY	10,286	3.979	0.015780
6	INTERNATIONAL ENDODONTIC JOURNAL	7,453	3.801	0.000666
7	JOURNAL OF PERIODONTOLOGY	16,306	3.742	0.010160
8	CLINICAL ORAL IMPLANTS RESEARCH	14,178	3.723	0.013970
9	Clinical Implant Dentistry and Related Research	4,496	3.396	0.008290
10	JOURNAL OF DENTISTRY	9,650	3.242	0.011330
11	Clinical Implant Dentistry and Related Research	3,633	3.097	0.008520
12	INTERNATIONAL ENDODONTIC JOURNAL	7,002	3.015	0.001650

Paper 1 (2020)

11. Paper 1

INTERNATIONAL
ENDODONTIC JOURNAL

doi:10.1111/iej.13232

Gaps at the interface between dentine and self-adhesive resin cement in post-endodontic restorations quantified in 3D by phase contrast-enhanced micro-CT

A. P. Soares[1], K. Bitter[1], A. Lagrange[1], A. Rack[2], H. Shemesh[3] & P. Zaslansky[1]

[1]Department of Operative and Preventive Dentistry, Charité - Universitätsmedizin Berlin, CharitéCentrum 3, Berlin, Germany; [2]ESRF-The European Synch, Grenoble, France; and [3]Department of Endodontology, Academic Centre for Dentistry Amsterdam, Amsterdam, The Netherlands

Abstract

Soares AP, Bitter K, Lagrange A, Rack A, Shemesh H, Zaslansky P. Gaps at the interface between dentine and self-adhesive resin cement in post-endodontic restorations quantified in 3D by phase contrast-enhanced micro-CT. *International Endodontic Journal*, **53**, 392–402, 2020.

Aim To assess the extent of gaps between root dentine and titanium or fibreglass post restorations following cementation with a self-adhesive resin cement.

Methodology Fourteen root filled maxillary central incisors restored with prefabricated posts made of Fibreglass ($n = 7$) or Titanium ($n = 7$) and cemented with RelyX Unicem 2 were imaged by rapid, high-resolution phase contrast-enhanced micro-CT (PCE-CT) in a synchrotron X-ray imaging facility (ID19, ESRF, 34 KeV, 0.65 μm pixel resolution). Reconstructions were used to measure canal, cement and post perimeters and cross-sectional areas and interfacial gaps at 0.1 mm increments in the root canal space, along the cervical region of the tooth. Remnants of endodontic sealer (AH Plus), when present, were also quantified. Mann–Whitney and 2-way ANOVA tests were used to compare findings within slices and between the two post groups. Pearson correlation coefficients (r) were determined between the interfacial gaps and the other measured parameters.

Results Clearly detectable gaps were found in 45% (±14%) of the interfaces between dentine and cement, along the canal in the cervical area of the tooth beneath the core. The length of interfacial gaps was moderately correlated to the canal cross-sectional area, to the canal perimeter and to the canal area filled by cement ($R = 0.52 \sim 0.55$, $P < 0.001$). There was no significant difference between samples with fibreglass or titanium ($P > 0.01$). Both post types had defect-free interfaces with cement. Endodontic sealer remnants were found on ~10% of the canal walls and were moderately correlated to the presence of gaps. Approximately 30% of the sealer-affected interfaces exhibited no detachment between dentine, sealer and cement.

Conclusions Self-adhesive cements had interfacial gaps along substantial regions of the root canal surface, which was not correlated with the amount of cement in the canal. PCE-CT proved to be an excellent non-destructive method to study root canal restorations of hydrated samples in 3D.

Keywords: cement debonding, phase contrast enhanced microcomputer tomography, post and core restoration, self-adhesive composite cement.

Received 10 April 2019; accepted 1 October 2019

Correspondence: Paul Zaslansky, Department of Operative and Preventive Dentistry, CharitéCentrum 3, Charité - Universitätsmedizin Berlin, Aßmannshauser Str. 4-6, 14197 Berlin, Germany (e-mail: paul.zaslansky@charite.de).

Introduction

Self-adhesive resin cements are used routinely to cement posts in root filled teeth. Their main advantage over other resin cements is that they adhere directly to the tooth structure without additional treatment steps of etching, conditioning or adhesive application (Burke *et al.* 2006). Indeed, standardized auto-mixing cement kits and thin intraoral tips have improved intracanal cement delivery (Opdam *et al.* 2002). Previous experiments found that the performance of self-adhesive resins is at least as good as other types of dental cements for post luting, using various methods of analysis including push-out bonding strength tests (Zicari *et al.* 2008, Pereira *et al.* 2014, Bitter *et al.* 2017). Despite their many advantages, self-adhesive cements have several limitations, such as occasional loss of retention and leakage that might lead to failure of the root canal treatment (Rasimick *et al.* 2010). Whilst some researchers (Kirkevang *et al.* 2000, Tavares *et al.* 2009) maintain that the apical seal is as important as the coronal seal for the longevity of the restoration, others claim that a well-sealed crown is more important (Ray & Trope 1995). Either way, it is accepted that a permeable restoration situated coronal to the root canal filling may lead to penetration of fluid and bacteria via microleakage (Neves *et al.* 2014). Due to the causative link between canal infections and periapical lesions (Kakehashi *et al.* 1966), interfacial gaps and microleakage in root canal restorations are undesirable and should be avoided (Heintze 2013, Jokstad 2016). Laboratory research has found that post cementation with self-adhesive resins has a larger number of voids in the cervical third of the root canal as compared with the middle or apical thirds (Uzun *et al.* 2016, Pedreira *et al.* 2016). All these observations raise concerns regarding the capacity of self-adhesive cements to create a defect-free, tight seal of the coronal third of the root canal.

Whilst it is desirable to attain a homogeneous seal between the restoration and the canal walls, there are no standardized ways to investigate and quantify the integrity of this resin–dentine interface. Push-out or pull-out mechanical tests are frequently used to assess the durability of post bond to canal dentine (Heintze 2013). However, the relationship between bond strength and structural integrity of the interface between dentine and cement is still uncertain (Rasimick *et al.* 2010) even though it is assumed that reduced strength values are suggestive of the presence of interfacial gaps at the canal walls.

Different approaches exist to directly examine the integrity of the interface between root filling components. Traditionally, interfaces between tooth tissues and fillings were visualized by serial sectioning and microscopy observations, for example stereo-, scanning electron- or confocal laser scanning-microscopes (Heintze 2013). Although informative, all these methods are destructive, as they require physical sectioning of the sample, which may inadvertently cause cracks to appear (Zaslansky *et al.* 2011). Indeed, the number of voids or the extent of interfacial spaces might be underestimated due to smear layer or sample preparation damage. An important approach to investigate interfacial gaps uses dyes to study microleakage (Neves *et al.* 2014). It is, however, controversial because of the questionable repeatability of this method. Tracer dyes such as organic colourants or silver nitrate require dye permeation through the filling (De Munck *et al.* 2005), which typically implies that 'through-and-through' gaps must exist (Hilton 2002). Such studies are frequently qualitative, typically focusing on one slice with little or no depth (three dimensional – 3D) information (Neves *et al.* 2014, Carrera *et al.* 2015). Overall, tracer infiltration is never uniform, and it frequently includes 'false-positive' findings as the dye either enters normal openings (e.g. dentine tubules or lateral canals) or reacts with the filling material leading to an overestimation of the presence of gaps (Shemesh *et al.* 2008, Kriznar *et al.* 2018).

Common to the methods listed above is that they are essentially destructive requiring cross-sections to expose 2D surfaces in the 3D volume of the tooth. However, for studying restoration interfaces, nondestructive 3D approaches that maintain and reveal the spatial integrity are of great value. Volume imaging techniques based on tomography have been used in interfacial gap studies (Bakhsh *et al.* 2011, Kwon & Park 2012, Carrera *et al.* 2015). Yet, visibility of details is a serious concern. Due to limited resolution, it is often difficult to distinguish between materials placed deep inside the dense structures of restored roots. The low density of most polymers precludes visualization of internal interfaces, to the extent that some researchers still use silver nitrate as a radiopaque tracer, to assess marginal gaps with laboratory micro-computed tomography (μCT) (Kwon & Park 2012, Neves *et al.* 2014). A different method, swept source optical coherence tomography, uses laser light rather than X-rays such that interfacial defects are easier to see (Nakagawa *et al.* 2013). Optical

coherence tomography is, however, limited by strong absorption by tooth/restoration tissues such that regions of interest must be situated near the detector (Nakagawa *et al.* 2013). Overall, the optical signal is rather weak, and the results become difficult to standardize (Bakhsh *et al.* 2011).

Phase contrast-enhanced μCT (PCE-CT) has matured to become a valuable 3D measurement method, well suited to provide accurate 3D information about the presence and extent of voids deep within root canal fillings (Zaslansky *et al.* 2011, Moinzadeh *et al.* 2016). Interfaces observed by PCE-CT are accentuated due to the use of partial coherence X-rays, leading to easier differentiation between material interfaces in root canal fillings. Thus, PCE-CT is useful to image, in 3D, interfacial gaps in a nondestructive manner and at micrometer resolution without requiring tracer penetration. PCE-CT requires the use of specialized high-flux X-ray facilities, able to produce 'laser-like' high-energy X-ray beams, known as synchrotrons (Moinzadeh *et al.* 2016). Such imaging allows fast scanning, that can be tuned to circumvent heating or dehydration of the samples. Yet synchrotron imaging entails overcoming the difficulties of accessing these research facilities, the restricted time allocated per experiment, and the large amount of data needing processing.

In the present *ex vivo* study, the aim was to nondestructively examine interfaces at the micrometer length scale, within intact post and core restorations placed in root filled teeth, made with a widely used self-adhesive resin cement (RelyX Unicem 2, 3M ESPE).

Materials and methods

Samples selection and endodontic preparation

Human maxillary central incisors ($n = 14$) were obtained with written informed consent and requirements of anonymity, under an ethics-approved protocol (EA4/102/14) by the Ethical Review Committee of the Charité Universitätsmedizin Berlin, Germany and stored in 0.5% chloramine T solution. The teeth selected contained no cavities, restorations or fractures and all had a single root 15 ± 1 mm long and a cervical diameter of 7 ± 0.5 mm. An impression of each crown (Silaplast Futur, Detax, Ettlingen, Germany) was obtained for later reconstruction of crown morphology, and all teeth were decoronated at the cervical margin using a water-cooled diamond band saw (Exact 312, Exakt, Norderstedt, Germany). During all treatment steps, roots were continuously kept wet using conventional dental chair waterlines. Each root canal was instrumented as follows: canal orifices were widened using Gates Glidden burs (no. 1-3, VDW, Munich, Germany). Working length was established with a size 10 K-file up to 1 mm from the anatomical apex. Canal instrumentation was carried out with the ProTaper Next System (Dentsply Sirona, Ballaigues, Switzerland) using files X1-X4 up to a final preparation of size 40, 0.07 taper. After each file, an intracanal irrigation of 1% sodium hypochlorite solution (Hedinger GmbH, Stuttgart, Germany) was applied using a Luer Syringe (Dentsply Sirona) and irrigating needles 30 gauge (Max-I-Probe, Dentsply Sirona). For final irrigation, a saline solution was used (Braun, Melsungen, Germany), followed by drying with paper points (ProTaper Next System X4 Paper Points, Dentsply Sirona). Each canal was filled with a single cone of matching gutta-percha (ProTaper Next System X4 gutta-percha cone, Dentsply Sirona) fitted to the working length and evenly coated with endodontic sealer (AH Plus, mixing ratio 1:1, Dentsply Sirona) uniformly spread on the canal walls up to ~7 mm from the apex. The filling was vertically condensed down to 7 mm below the cervical margin using the Calamus Dual System (Dentsply Sirona). Each root was temporarily sealed with Teflon tape covered by a thin layer of temporary filling and stored moist in a water-tight vial for final restoration within 24 h.

Post build-up and restoration

Following storage, gutta-percha and dentine were removed from the canal using standardized pilot and reamer drills (ER System Pilot bur and system reamer, stainless steel, size 090 Komet, Lemgo, Germany) under constant water irrigation to a depth of 9 mm. In this manner, it was possible to ensure that at least 5 mm of apical seal of the root filling remained intact whilst creating standardized post spaces in the coronal region. Each canal was examined under a stereomicroscope (WilD M3Z, Wild Heerbrug, Heerbrug, Switzerland) to identify and remove any visible remaining gutta-percha and all signs of endodontic sealer. Thereafter, 1% sodium hypochlorite was used and flushed with distilled water, followed by blot-drying with paper cones, as recommended by the cement manufacturer. The teeth, divided into two groups, were immediately treated: 7 teeth in group 1 were

restored with a fibreglass post (Dentin Post size 090, Komet, Lemgo, Germany) as follows: each post was cleaned with 96% ethanol, silanized (Ceramic Bond, Voco, Cuxhafen, Germany) coated with and cemented using the dual-curing self-adhesive resin cement RelyX Unicem 2 (Automix delivery system, 3M ESPE Dental Products, St Paul, MN, USA). Cement was applied into the root canal using mixing tips coupled with the dedicated intraoral application kit tips. The second group of 7 teeth was similarly restored, but using titanium posts (Kopfstift Titanium Post size 090, Komet). For both groups, chemical polymerization was enhanced by light curing, illuminating the filled canal orifice with a light cure LED (Valo Corded, Ultradent Products Inc, South Jordan, UT, USA) for 40 s. Following polymerization, excess cement was removed with a sharp blade. Each tooth crown was immediately restored with composite (Rebilda DC Quickmix, Voco, Cuxhaven, Germany): the exposed tooth cervical area was etched with phosphoric acid 37% (Orbi Flow, Orbis Dental, Münster, Germany), washed and briefly air-dried. An adhesive system (Futurabond U Single Dose, Voco) was applied for 20 s, agitated with a microbrush according to manufacturer instructions, dried for 5 s and light cured for 10 s. Automix tips (Mixing Tips type 14) containing the dual-curing composite core build-up material Rebilda DC were used to coat the post and dentine surfaces. Thereafter, the corresponding dental impression of each tooth was filled with composite and placed onto the root to recreate the original crown shape. Curing was enhanced by exposing the apical margins of the restoration at the impression margins to light cure for 40 s. After 5 min, the silicone impression moulds were removed, crowns were further light cured for 40 s, trimmed, polished and the teeth were returned to the airtight vials for wet storage for one week until imaging.

Imaging and reconstruction

Prior to imaging, each sample was mounted in a PVA vial (Micro tube 2ml, Sarstedt, Nümbrecht, Germany), centrally stabilized in styropore pieces padded with moist foam to maintain a humid atmosphere in the air surrounding the samples.

Laboratory micro-CT (Laboratory μCT) (Skyscan 1172, Bruker micro CT, Kontich, Belgium) was used to image the specimens at moderate resolution (16 μm pixel size, 700 ms exposure time). Following reconstruction (NRecon 1.7.1.0, Bruker micro CT) the 3D architectures of the restorations were examined in both 2D and 3D (Fig. 1a) (ImageJ 1.52d, National Institutes of Health, Bethesda, MD, USA; CTvox, Bruker micro CT). The cervical areas, just beneath each core, were selected for high-resolution imaging in a synchrotron. Samples were scanned on beamline ID19 of the European Synchrotron Radiation Facility (ESRF, Grenoble, France) using inline propagation-based contrast enhancement. An X-ray photon energy of 34 keV with partial coherence used to minimize absorption and induce phase contrast enhancement. The imaging system consisted of a pco.edge camera (PCO AG, Kelheim, Germany), LSO scintillator in a

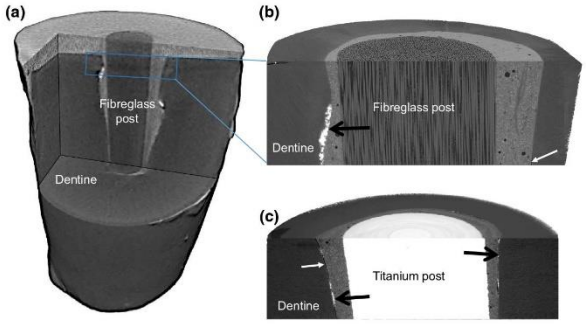

Figure 1 Low-resolution Laboratory μCT images versus high-resolution PCE-CT: (a) Laboratory μCT is useful for scans of the entire root, containing the region of interest (e.g. blue marked box) at moderate resolution. High-resolution scans by PCE-CT provided sub-micrometer resolution data of teeth restored with (b) fibre and (c) titanium posts. Note the impressive contrast and high level of detail. White arrows identify voids between dentine and cement. Black arrows show remnants of endodontic sealer.

custom-made imaging system (OptiquePeter, Lentilly, France) with an effective pixel size of 0.65 μm. PCE-CTs were obtained using a sample-detector distance of 33 mm. Each sample was mounted on the high-resolution rotation stage and in each scan, a total of 4900 radiographic projections were recorded (200 ms exposure times) whilst continuously rotating the samples by 360° (using a horizontal stitching mode to image samples wider than the field of view), requiring approximately 16 min per scan. During all stages of imaging, the samples were maintained in airtight, sealed vials maintaining saturated humidity conditions (droplets visibly condensing on the vial walls) under a constant hutch temperature of 23 °C. ESRF in-house code was used to reconstruct the data, enhancing contrast in the radiographs by means of Paganin-based filtering (delta/beta ratio of 200, Mirone *et al.* 2014).

Image processing and parameters quantification

The high-resolution reconstructed datasets were visualized using ImageJ and CTvox, and topographies typically contained more than 2100 slices along the post axis, occupying more than 80–90 Gigabytes each. Example 3D reconstructions are shown in Figs. 1 and 2 with corresponding high-resolution cross-sectional and longitudinal slices shown in Fig. 2. For data analysis, $n = 13$ artefact-free reconstructions were quantified so as to compare integrity, interface architecture, gaps and internal voids (the 14th PCE-CT scan failed due to unrecoverable data loss). The 3D datasets were reduced to produce 5 μm thick slices using the minimum intensity projection of 8 neighbouring sub-micrometer slices (Z project function of ImageJ). Slices 100 μm apart were then compared within the cervical area of each tooth, at increasing distances below the apical margins of the core build-up. Slices at identical depths of all teeth were selected for further processing for both intra- and inter-tooth comparisons. Analysis included measurements of the canal, cement and post perimeters as well as the cross-sectional areas, all performed by a single evaluator (AS). The total length of observed interfacial gaps between root and restoration materials was recorded. The length of remnants of endodontic sealer (AH Plus) on the canal perimeter was also measured. Data were used to derive four measures of quality: % canal area filled with post and with cement, % interfacial gaps and % canal perimeter covered by remnants of sealer.

Statistical analysis

Data were tabulated and analysed using SciDAVis (version 1.23, Souceforge, Boston, MA, USA). The Mann–Whitney test was used to compare the length of interfacial gaps and percentage of interfacial gaps between groups, with significance values attributed to $P < 0.01$. The length of interfacial gaps in the uppermost and lowermost three slices of each sample was compared with a 2-way ANOVA using the *t*-Test (LSD) post hoc test. Pearson correlation coefficient (r) was determined between length of interfacial gap and different parameters (canal area, canal perimeter, cement area, post area, post perimeter and length of the perimeter with sealer remnants).

Results

Laboratory μCT reproduced all the components of the post restoration within the root, whereas the actual gaps, voids and sealer were only fully revealed by the enhanced contrast and sub-micrometer resolution of PCE-CT. As shown by 3D renderings (Fig. 1) and by virtual cross-sectional and longitudinal slices (Fig. 2), impressive details are revealed in each of the layers comprising the specimens (Videos S1 & S2). PCE-CT revealed dentinal tubules in dentine, filler particles in the cement and even single glass fibres of the fibreglass post. The high-quality images generated with PCE-CT are comparable with micrographs obtained with scanning electron microscopy (Figure S1). Importantly, at the energy of the experiment, PCE-CT has high transmission values thus undergoing little absorption by the sample. The phase contrast enhancement highlights the presence of gaps at the interfaces of self-adhesive resin cements and in other cements (Figure S2). Indeed, PCE-CT reliably detects flaws and other features at the interface between different biomaterials (Appendix S1, Cloetens *et al.* 1997) and the canal walls. In fact, the enhanced contrast highlights porosity and inclusions in pores

Figure 2 Slices derived from within the 3D data of a Fibreglass post (I) and a Titanium post (II) restored root: (a) Slices along the blue planes indicated in the 3D datasets reveal inclusions, gaps and delamination in both (b) cross-sectional and (c) longitudinal slices. White arrows identify typical interfacial gaps and black arrows point to sealer remnants.

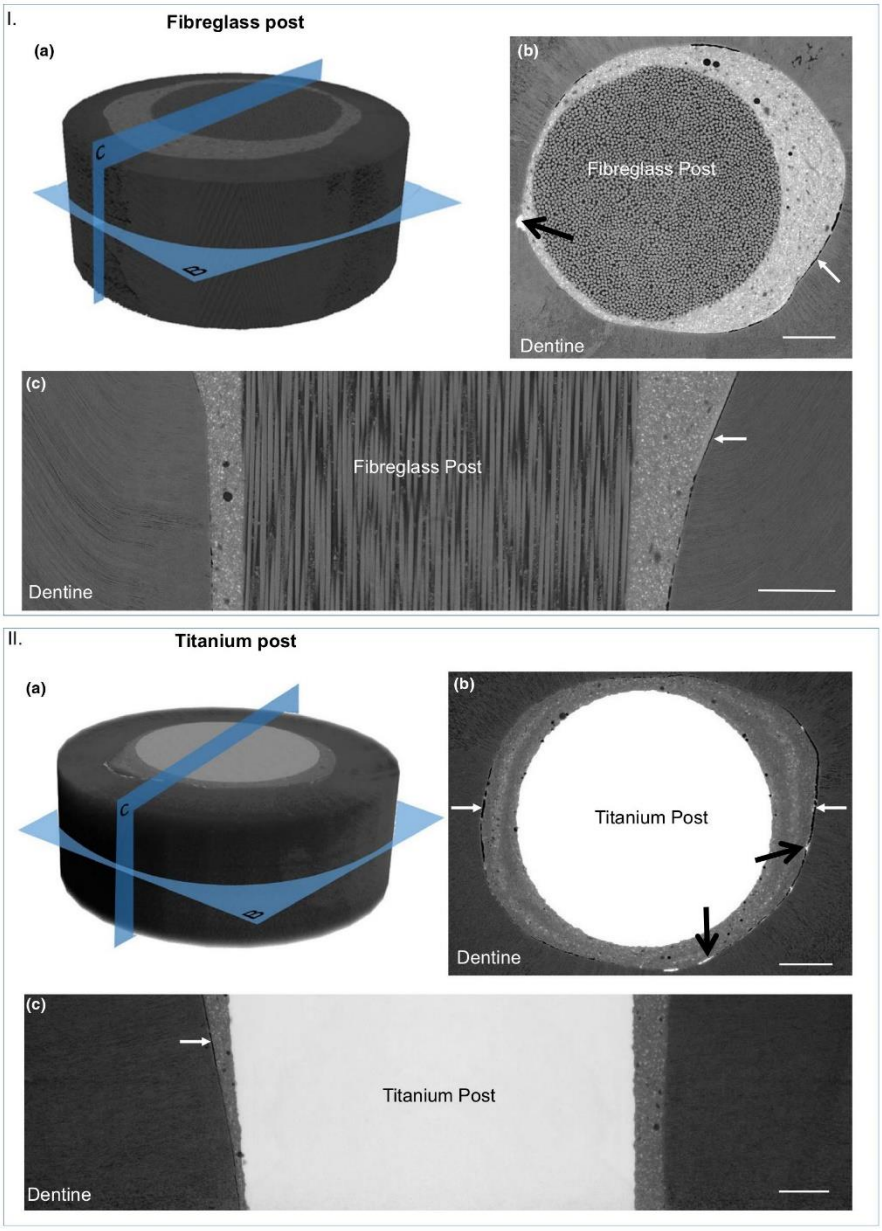

(Figure S3). Examination of all scanned teeth showed that slices in the 3D data clearly show how the post rarely takes up a central position in the cervical area of the canal. Consequently, all slices exhibit an uneven distribution of the cement on the different sides of the post (Fig. 2, Videos S1 & S2). Sporadically, water droplets were seen, yet none of the samples had any signs of cracking of dentine, indicative that the samples maintained hydration for the entire duration of the experiment thus avoiding dehydration artefacts (Shemesh *et al.* 2018).

Geometric measurements performed on each slice along the axis of the filling reveal values for area and length estimates of the canal, filling and discontinuities at the interfaces. Average values as well as any trends in the data such as the expected taper in the cervical canal perimeter/area from the most coronal to apical region, are given in Table S1. The measurements were used to derive the percentage of the filled canal cross-section and percentage of imperfections (gaps and sealer presence) observed at the dentine–cement interfaces, as depicted in Figure 3. The results reveal expected increases in the canal areas filled by the post (Fig. 3a) and decreases in canal area filled by cement (Fig. 3b). The trend in the data and ratios of cement to canal areas with increasing depths are shown in Figure S4. Interfacial gaps were observed in ~45% of the contact area between dentine and cement revealing that discontinuities were uniformly present along the cervical canal in all of the samples (Fig. 3c). There was no significant difference ($P > 0.01$) in the % length of gaps between the three uppermost slices and the three lowermost slices of all samples, further showing the uniformity of discontinuities along the imaged canal area and between groups. No interfacial gaps were identified between cement and post in any of the samples (data not shown). At the interface between dentine and cement, many of the slices exhibited some remnants of the epoxy based endodontic sealer (AH Plus), always in intimate contact to dentine in the canal walls but not always associated with cement–dentine discontinuities. Figure 3d shows that approximately 10% of all canal perimeters both coronally and apically were contaminated with sealer, exhibiting a fairly even distribution with depth. There was a moderately positive correlation (Pearson correlation test, $r = 0.52 \sim 0.55$, $P < 0.001$) between interfacial gaps and sealer presence, and also with the canal perimeter (Figure S5), the canal area and the cement area (Table S1). No significant differences were observed in the length of interfacial gaps or in the % of interfacial gaps between groups restored with fibreglass and titanium posts (Table S1, $P > 0.01$).

Discussion

Self-adhesive resin cements are commonly employed for post cementation, but post dislodgment remains a major, poorly understood mode of failure (Rasimick *et al.* 2010). Of this group of materials, RelyX Unicem 2 has a long good track record and is widely used. The results reveal that regardless of the type of post and the depth to which it is placed, almost half of the interface surface between the cement and the root canal walls exhibited gaps. The observed micron-sized discontinuities are extremely narrow (see Fig. 2 and Figure S2), which is why they are best observed in intact teeth using reasonably high energy ($E > 30$ keV) PCE-CT. The restorations quantified in this work were performed according to manufacturer instructions and under standardized, idealized, reproducible conditions in the laboratory. They were further imaged swiftly and under fully hydrated stable conditions (watertight vials). Dehydration, contamination, incomplete adherence to treatment protocol, premature mechanical loading or patient related variability as possible causes for the observed compromised integrity of the restorations can therefore be ruled out. A closer examination of the results reveals moderately positive correlations between the presence of interfacial voids and the parameters 'cement cross-sectional area', 'canal perimeter' and 'canal area'. However, when the interfacial gaps are normalized by the canal perimeter, there is no difference by depth as seen clearly in Figure 3c. This is noteworthy since the cement cross-sectional area decreases as the percent of canal filled with post increases (Figure S2). Consequently, the extent of interfacial gaps is not affected by the amount of cement present in the canal. Indeed Li *et al.* (2008) showed using computer simulations that the mass of resin and restoration diameter negligibly affect the stress state at the interface between dental composites and restoration margins. The mass of cement and the root canal surface dimensions must therefore be ruled out as main reasons for gap formation at the interfaces between dentine and cement during setting. The C-factor (ratio of bonded to free surface area) in these restorations is very high, as most surfaces are bonded. It is thus possible

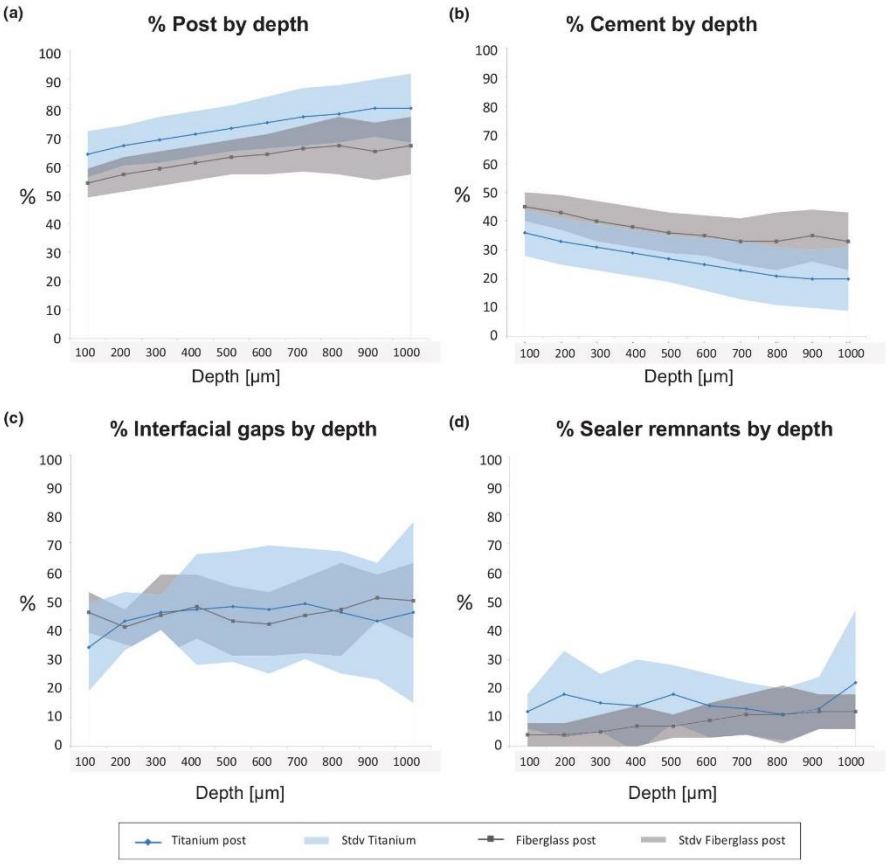

Figure 3 Trends in % filled and % gaps/sealer in titanium and fibrepost restored teeth: (a) % Post area (Post area/Canal area), (b) % Cement area (Cement area/Canal area), (c) % interfacial gaps between cement and dentine (Gaps perimeter/Canal perimeter) and (d) % remaining sealer on the perimeter of the canal walls (Sealer remnant perimeter/Canal perimeter) at increasing depths beneath the apical margin of the core buildup.

that RelyX Unicem 2 shrinkage, although low when compared to other self-adhesive resin cements (Kitzmuller *et al.* 2011), leads to stresses that develop sooner than, or are higher than the early established bond strength between the setting cement and the root dentine. Such localized stresses may then lead to widespread detachment, concentrated at the weakest interface, namely between cement and dentine along the root surface. Further work is needed to accept or refute these speculations.

The PCE-CT measurements focused on the coronal, outermost part of the cemented post, corresponding to the cervical first millimetre beneath the core build-up. The cervical tooth region exhibits reduced mass of remaining healthy dentine (due to caries or as a result of root canal treatment) and must therefore experience elevated stresses, due to tooth loading and bending during oral function. Consequently, besides resistance to bacteria and biofilm ingrowth, an important reason for the dentist to attempt to establish a

defect-free cervical restoration is to create a solid structure to optimally resist mastication induced stress. The lack of homogeneous continuous interfaces between tooth and restoration questions the capacity of self-adhesive resin cements to create a so-called endodontic 'monoblock' (Tay & Pashley 2007), free of structural defects, which is essential to establish the maximal mechanical resistance to masticatory load. It is proposed that immediately after construction, thin extended gaps appear between the dentine and the resin cement at the time of placement. These then appear to remain as flaws in the constructed post-endodontic restoration. Such pre-existing cracks might progress with time either due to fatigue related to cyclic loading or following excessive overload (e.g. biting on hard bone inside soft meat) after which the post may become dislodged.

In addition to gaps, sealer remnants were observed along the canal in most samples, demonstrating that despite meticulous surface preparation and careful inspection prior to post placement, approximately 10% of the prepared canal surfaces remain 'contaminated' by the sealer used (AH Plus, Figure S3). The degree to which sealer remnants remain in the canal might be a function of the protocol used for canal preparation. Complete removal of AH Plus is extremely difficult using chemical solvents (Kuga *et al.* 2013), and therefore, it is probably best to reduce contact between the sealer and the coronal parts of the root canal. In fact, complete elimination of the sealer might require substantial removal of sound, healthy dentine, which is difficult to justify and is certain to jeopardize the root and thus the entire treatment outcome. There was only moderate correlation between gaps and the presence of endodontic sealer (Table S1). This suggests that root surface contamination, such as sealer remnants, debris from canal instrumentation, entrapped air or biofilm (not properly observable with PCE-CT imaging), might obstruct direct contact between self-adhesive cements and tooth tissues. Note, however, that 30% of the areas where there were clear signs of endodontic sealer remnants (data not shown) showed no interfacial gaps between the sealer, cement and dentine. This suggests that AH Plus does not prevent RelyX Unicem 2 from forming a gap-free contact with the sealer. In fact, previous work has clearly shown bond formation between sealer and cement (Cecchin *et al.* 2011). Overall, these findings suggest that complete removal of sealer is desirable, or better still, that new application methods/protocols are needed, designed to protect root dentine from root filling sealer contamination in coronal regions of the canal, in preparation for improving subsequent post and core construction. Additional studies are needed to address this topic.

A homogenous interface between cement and the post is necessary for the post-and-core restoration stability (Prado *et al.* 2017). Both fibreglass and titanium posts are widely used, although, due to limited studies on the subject, titanium posts are associated with greater clinical success rates (Kramer *et al.* 2019). RelyX Unicem 2 showed homogeneity of bonding to both titanium and fibreglass posts in all samples at all depths. Note that the surfaces of both types of posts were pretreated; whereas the titanium post is prefabricated with a micro-rough surface, the fibreglass posts were treated with silane immediately before cementation.

This work showcases the advantages of PCE-CT for imaging interfaces within root canal fillings (Moinzadeh *et al.* 2016). Details were revealed nondestructively and without the use of dyes, demonstrating gaps and delamination at sub-micrometer resolution. The fast scans (3 ~ 4 scans per hour) of samples mounted in controlled humid environments with minimal absorption due to the use of rather high energy (34 keV) ensure minimal radiation or dehydration damage. Consequently, interfacial voids could be measured in a truly nondestructive manner, in 3D, free of any sample preparation artefacts. Furthermore, the PCE-CT data delivers much higher resolution and contrast than that available by Laboratory μCT; hence, the use of both methods for this work delivers data that was previously not available.

The present work is not without limitations. Synchrotron-based micro tomography is not easily accessible, which limits the number of samples that can be imaged per experiment. Furthermore, in high-resolution imaging, the field of view is limited and imaging processing and reconstruction require massive computational power and processing of huge amounts of data, which restricts the regions that can realistically be investigated in a single experiment. Analysis of the 3D data is also challenging. Future artificial intelligence and machine learning approaches may pave the way to distinguish between different states of the material imaged (liquid resin, water or debris in voids) or facilitate identifying flaws in 3D as a step to improving treatment protocols.

Conclusions

The interface between RelyX Unicem 2 cemented posts and coronal root dentine was associated with gaps

extending 45% of the total dentine–resin surfaces. The length of the gaps moderately correlate with the canal perimeter and the canal and cement cross-sectional areas. The percentage of interfacial gaps did not vary along the imaged canal depth, suggesting a lack of relationship between cement thickness and gap formation at the interfaces. Approximately 10% of the root canal walls revealed traces of sealer. There were no interfacial gaps between either the fibreglass or the titanium posts and cement. PCE-CT made it possible to nondestructively quantify the spatial relations and discontinuities between all phases of the moist root canal cemented post.

Acknowledgement

The experiments were performed on beamline ID19 of the European Synchrotron Radiation Facility (ESRF), Grenoble, France. We are thankful for a supplementary figure obtained for comparison with experimental this data, with the help and support of Andrew King from PSICHE Beamline, Soleil Synchrotron (Paris, France).

Conflict of interest

Dr. Prates Soares reports funding to support her PhD from the Elsa Neumann Stipendium des Landes Berlin, making it possible to conduct the study. The other authors have stated explicitly that there are no conflicts of interest in connection with this article.

REFERENCES

Bakhsh TA, Sadr A, Shimada Y, Tagami J, Sumi Y (2011) Non-invasive quantification of resin-dentin interfacial gaps using optical coherence tomography: validation against confocal microscopy. *Dental Materials* **27**, 915–25.

Bitter K, Maletic A, Neumann K, Breschi L, Sterzenbach G, Taschner M (2017) Adhesive durability inside the root canal using self-adhesive resin cements for luting fiber posts. *Operative Dentistry* **42**, 167–76.

Burke FJ, Crisp RJ, Richter B (2006) A practice-based evaluation of the handling of a new self-adhesive universal resin luting material. *International Dental Journal* **56**, 142–6.

Carrera CA, Lan C, Escobar-Sanabria D, et al. (2015) The use of micro-CT with image segmentation to quantify leakage in dental restorations. *Dental Materials* **31**, 382–90.

Cecchin D, Farina AP, Souza MA, Carlini-Junior B, Ferraz CC (2011) Effect of root canal sealers on bond strength of fiberglass posts cemented with self-adhesive resin cements. *International Endodontic Journal* **44**, 314–20.

Cloetens P, Pateyron-Salomé M, Buffière JY, et al. (1997) Observation of microstructure and damage in materials by phase sensitive radiography and tomography. *Journal of Applied Physics* **81**, 5878–86.

De Munck J, Van Landuyt K, Peumans M, et al. (2005) A critical review of the durability of adhesion to tooth tissue: methods and results. *Journal of Dental Research* **84**, 118–32.

Heintze SD (2013) Clinical relevance of tests on bond strength, microleakage and marginal adaptation. *Dental Materials* **29**, 59–84.

Hilton TJ (2002) Can modern restorative procedures and materials reliably seal cavities? In vitro investigations. Part 2. *American Journal of Dentistry* **15**, 279–89.

Jokstad A (2016) Secondary caries and microleakage. *Dental Materials* **32**, 11–25.

Kakehashi S, Stanley HR, Fitzgerald RJ (1966) The effects of surgical exposures of dental pulps in germfree and conventional laboratory rats. *Journal Southern California Dental Association* **34**, 449–51.

Kirkevang L, Ørstavik D, Hörsted-Bindslev P, Wenzel A (2000) Periapical status and quality of root fillings and coronal restorations in a Danish population. *International Endodontic Journal* **33**, 509–15.

Kitzmuller K, Graf A, Watts D, Schedle A (2011) A Setting kinetics and shrinkage of self-adhesive resin cements depend on cure-mode and temperature. *Dental Materials* **27**, 544–51.

Kramer EJ, Meyer-Lueckel H, Wolf TG, Schwendicke F, Naumann M, Wierichs RJ (2019) Success and survival of post-restorations: six-year results of a prospective observational practice-based clinical study. *International Endodontic Journal* **52**, 569–78.

Kriznar I, Zanini F, Fidler A (2018) Presentation of gaps around endodontic access cavity restoration by phase contrast-enhanced micro-CT. *Clinical Oral Investigations* **1**, 1–11.

Kuga MC, Faria G, Rossi MA, et al. (2013) Persistence of epoxy-based sealer residues in dentin treated with different chemical removal protocols. *Scanning* **35**, 17–21.

Kwon OH, Park SH (2012) Evaluation of internal adaptation of dental adhesive restorations using Micro-CT. *Restorative Dental Endodontics* **37**, 41–9.

Li J, Li H, Fok SL (2008) A mathematical analysis of shrinkage stress development in dental composite restorations during resin polymerization. *Dental Materials* **24**, 923–31.

Mirone A, Brun E, Gouillart E, Tafforeau P, Kieffer J (2014) The PyHST2 hybrid distributed code for high speed tomographic reconstruction with iterative reconstruction and a priori knowledge capabilities. *Nuclear Instruments and Methods in Physics Research Section B: Beam Interactions with Materials and Atoms* **324**, 41–8.

Moinzadeh AT, Farack L, Wilde F, Shemesh H, Zaslansky P (2016) Synchrotron-based Phase Contrast-enhanced Micro-Computed Tomography Reveals Delaminations and Material Tearing in Water-expandable Root Fillings Ex Vivo. *Journal of Endodontics* **42**, 776–81.

Nakagawa H, Sadr A, Shimada Y, Tagami J, Sumi Y (2013) Validation of swept source optical coherence tomography (SS-OCT) for the diagnosis of smooth surface caries in vitro. *Journal of Dentistry* **41**, 80–9.

Neves AA, Jaecques S, Van Ende A, et al. (2014) 3D-microleakage assessment of adhesive interfaces: exploratory findings by μCT. *Dental Materials* **30**, 799–807.

Opdam NJ, Roeters JJ, Joosten M, Veeke O (2002) Porosities and voids in Class I restorations placed by six operators using a packable or syringeable composite. *Dental Materials* **18**, 58–63.

Pedreira AP, D'Alpino PH, Pereira PN, et al. (2016) Effects of the application techniques of self-adhesive resin cements on the interfacial integrity and bond strength of fiber posts to dentin. *Journal of Applied Oral Science* **24**, 437–46.

Pereira JR, Da Rosa RA, Do Valle AL, Ghizoni JS, So MV, Shiratori FK (2014) The influence of different cements on the pull-out bond strength of fiber posts. *The Journal of Prosthetic Dentistry* **112**, 59–63.

Prado M, Marques JN, Pereira GD, da Silva EM, Simão RA (2017) Evaluation of different surface treatments on fiber post cemented with a self-adhesive system. *Materials Science & Engineering C-Materials for Biological Applications* **77**, 257–62.

Rasimick BJ, Wan J, Musikant BL, Deutsch AS (2010) A review of failure modes in teeth restored with adhesively luted endodontic dowels. *Journal of Prosthodontics* **19**, 639–46.

Ray HA, Trope M (1995) Periapical status of endodontically treated teeth in relation to the technical quality of the root filling and the coronal restoration. *International endodontic journal* **28**, 12–8.

Shemesh H, Souza EM, Wu MK, Wesselink PR (2008) Glucose reactivity with filling materials as a limitation for using the glucose leakage model. *International Endodontic Journal* **41**, 869–72.

Shemesh H, Lindtner T, Portoles CA, Zaslansky P (2018) Dehydration Induces Cracking in Root Dentin Irrespective of Instrumentation: A Two-dimensional and Three-dimensional Study. *Journal of Endodontics* **44**, 120–5.

Tavares PB, Bonte E, Boukpessi T, Siqueira JF Jr, Lasfargues JJ (2009) Prevalence of apical periodontitis in root canal-treated teeth from an urban French population: influence of the quality of root canal fillings and coronal restorations. *Journal of Endodontics* **35**, 810–3.

Tay FR, Pashley DH (2007) Monoblocks in root canals: a hypothetical or a tangible goal. *Journal of Endodontics* **33**, 391–8.

Uzun IH, Malkoç MA, Keleş A, Öğreten AT (2016) 3D micro-CT analysis of void formations and push-out bonding strength of resin cements used for fiber post cementation. *The Journal of Advanced Prosthodontics* **8**, 101–9.

Zaslansky P, Fratzl P, Rack A, Wu MK, Wesselink PR, Shemesh H (2011) Identification of root filling interfaces by microscopy and tomography methods. *International Endodontic Journal* **44**, 395–401.

Zicari F, Coutinho E, De Munck J, et al. (2008) Bonding effectiveness and sealing ability of fiber-post bonding. *Dental Materials* **24**, 967–77.

Supporting Information

Additional Supporting Information may be found in the online version of this article:

Appendix S1. Non-destructive microscopic 3D imaging of root canal fillings by PCE-CT

Figure S1. High compatibility between both resolution and contrast observed near RelyX Unicem2 cemented titanium and fiberglass posts, imaged first by PCE-CT followed by destructive SEM imaging.

Figure S2. High-resolution PCE-CT interface gaps observed between dentin and four types of post-cementation material: (a) self-adhesive resin cement (RelyX Unicem 2), (b) resin modified glass ionomer cement (RMGIC), (c) glass ionomer cement (GIC), (d) core composite bonded with a universal adhesive system.

Figure S3. High-resolution PCE-CT reveals interface features including: traces of tubules identifiable in dentin, interfacial gaps, zones with remnants of sealer, air bubbles in the cement layer and a water droplet residing inside a large air bubble (appearing black).

Figure S4. Boxplot of the ratios between cement area and canal area along the samples (depth in μm), showcasing a decrease in the cement filled area along the canal depth.

Figure S5. Plot of the canal perimeter (mm) versus the interfacial gaps length of the canal (mm), showing a moderately positive correlation (r: 0.5493, $P < 0.01$) between both measurements.

Table S1. Means and standard deviations of each measured parameter for both groups (titanium and fiberglass posts), tabulated by depth (every 100 μm).

Video S1. Slices along the axis of a typical root canal filling restored with a fiberglass post.

Video S2. Slices along the axis of a typical root canal filling restored with a titanium post.

Gaps at the interface between dentin and self-adhesive resin cement in post endodontic restorations quantified in 3D by phase contrast-enhanced micro-CT

Supporting Information:

Phase contrast-enhanced micro-CT (PCE-CT) reveals extensive details in 3D, exposing subtle changes and discontinuities in material density (cracks, voids, gaps (Cloetens *et al.* 1997), comparable to observations by electron microscopy. To verify the capacity of PCE-CT to reveal interfacial gaps in root canal restorations stored and imaged in a fully hydrated, humidity and temperature controlled environment, several validation experiments were performed:

1. Direct comparison between PCE-CT and scanning electron microscopy:

Direct comparison between conventional microscopy and PCE-CT is only possible by destructive sample preparation. Two PCE-CT imaged samples, one from each group, were cross sectioned with a water-cooled diamond band saw (Exact 312, Exakt, Norderstedt, Germany). The slices were dehydrated using a graded series of ethanol solutions (30 – 100%), followed by critical point drying (CPD 030, Baltec, Balzers, Lichtenstein). The samples were imaged by backscattered electron microscopy at 10 kV (Phenom XL, Thermo Fisher Scientific, Massachusetts, USA). The PCE-CT tomographic data of the wet-imaged samples described in the main text were examined to find identical regions to those exposed by the cross-sectional slicing.

Despite careful dehydration, the large cross-sections imaged by SEM suffer from cracks produced during sample preparation. Identical regions of one fiberglass post and one titanium post are shown in Supplementary Fig. 2. Whereas identical features and comparable contrasts are observed at a magnification of 300x, the SEM prepared samples are severely damaged due to slicing (Zaslansky *et al.* 2011) and dehydration (Shemesh *et al.* 2018) highlighting the advantage of the PCE-CT method for non-destructive imaging of gaps in root-filled teeth (Moinzadeh *et al.* 2016).

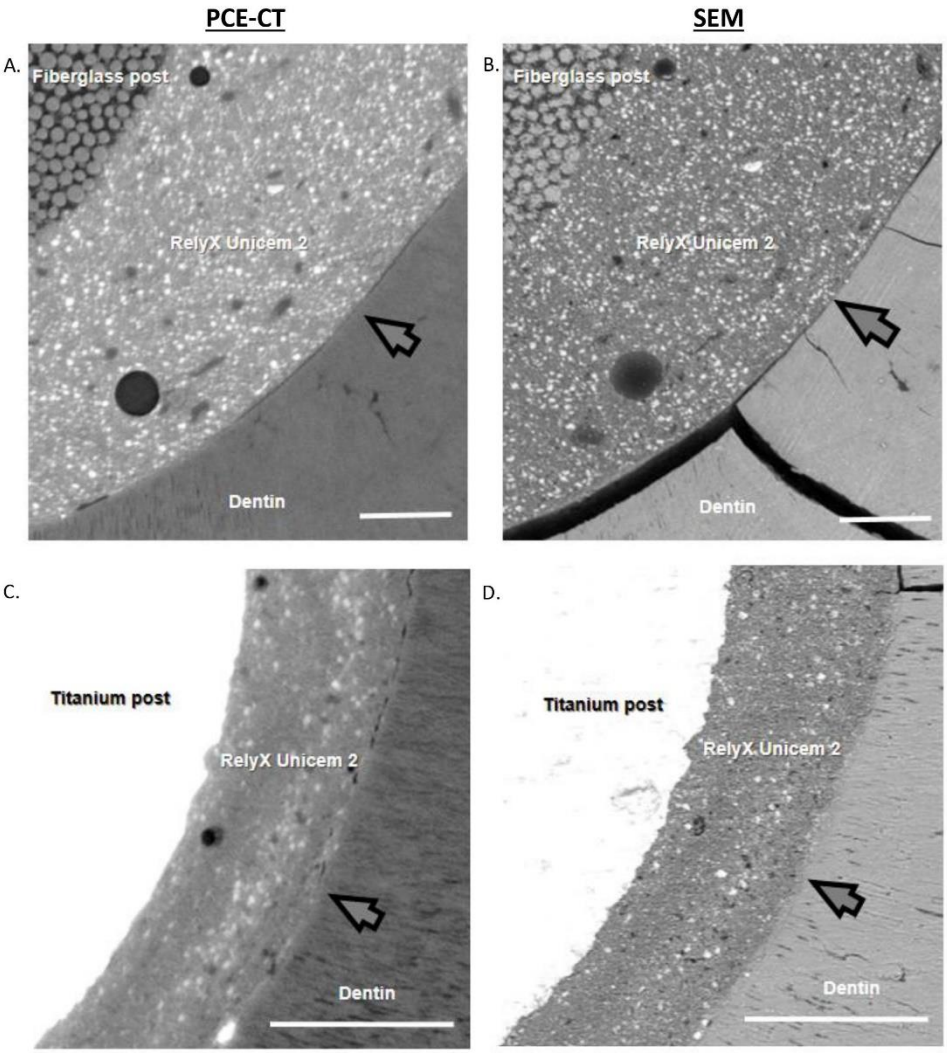

Supplementary Figure 1: High compatibility between both resolution and contrast observed near RelyX Unicem2 cemented titanium and fiberglass posts, imaged first by PCE-CT followed by destructive SEM imaging. Note silhouettes of dentin tubules, dentin-cement interface, voids and particles in the cement. Areas, where the interface is continuous (arrow) can be observed both with PCE-CT and SEM. Scale bar 100 µm.

2. PCE-CT interface imaging of materials and gaps between cement and root dentin:

In a pilot study, PCE-CT was used to image four classes of materials employed for post cementation: Glass Ionomer cement (GIC – Fuji I, GC Europe), resin-modified GIC (RMGIC – Ketac Cem Plus Automix, 3M ESPE), self-adhesive cement (RelyX Unicem 2) with self-etching universal adhesive (Futurabond U, VOCO) and core composite (Rebilda DC, VOCO). The cervical first millimeter of both samples were scanned one week after fabrication. All samples other than GIC were imaged for PCE-CT as described in the main text on ID19 of the ESRF. The GIC sample was similarly imaged on the PSICHE Beamline in the Soleil Synchrotron (Paris, France), using analogous phase contrast enhanced imaging conditions. All data was reconstructed using PyHST as described in the main text employing Paganin filtering.

Supplementary Fig. 1 shows typical views of cracks and gaps revealed by PCE-CT, as previously demonstrated (Zaslansky *et al.* 2011). Tubule silhouettes are often seen in dentine, the cements reveal inclusion particles and all show interfacial gaps.

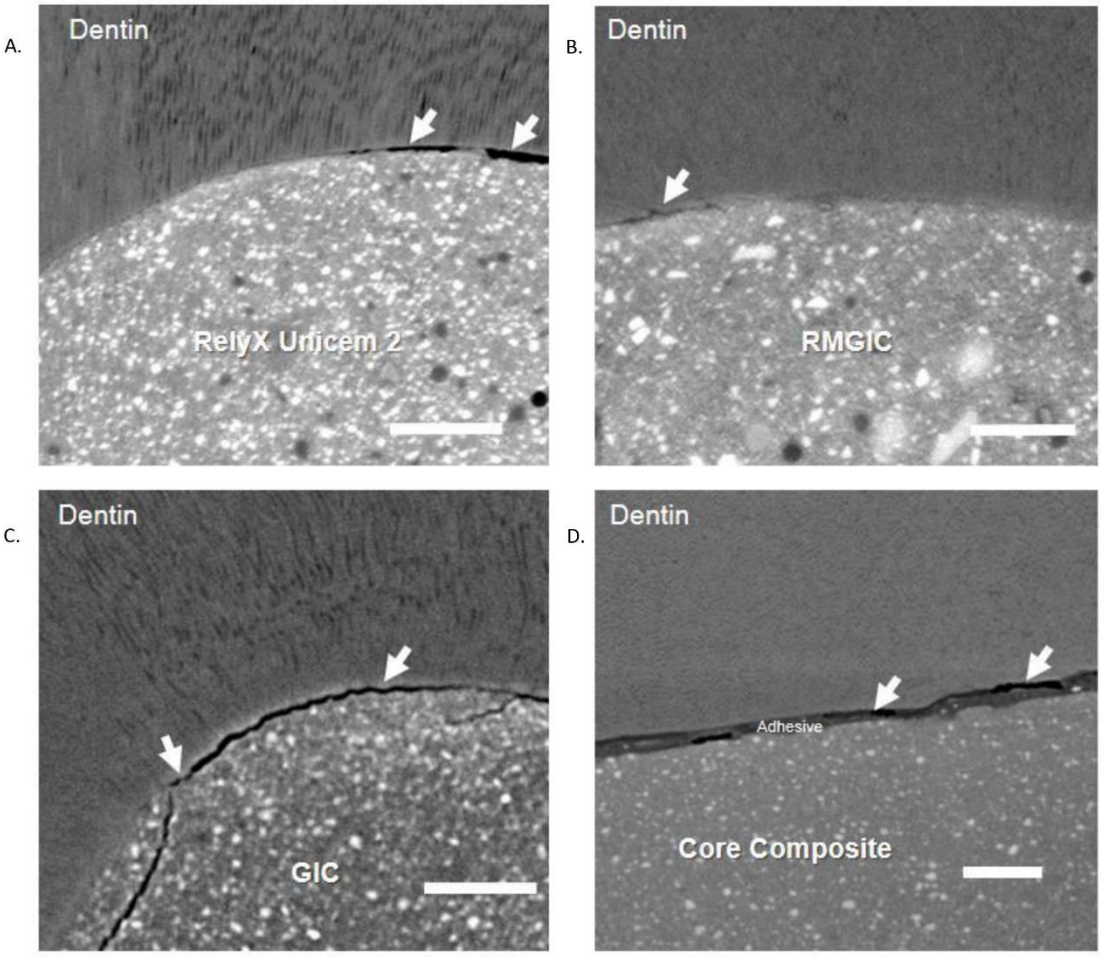

Supplementary Figure 2: High-resolution PCE-CT interface gaps (white arrows) observed between dentin and four types of post-cementation material: A. self-adhesive resin cement (RelyX Unicem 2), B. Resin modified Glass Ionomer Cement (RMGIC), C. Glass Ionomer Cement (GIC), D. Core Composite bonded with a Universal Adhesive System. Scale bar 100 µm.

3. Contrast-enhancement reveals extensive details and water drops near cemented posts:

The datasets were rich in a wide range of structural details from each sample, as demonstrated in Supplementary Fig 3 and in the Supplementary movies 1 & 2. An included air bubble (void) in the cement layer surrounding a fiberglass post is seen to contain a low-density water droplet attesting to the wet state of the sample. Large gaps and sealer remnants are observed at the interface between dentin and resin near a titanium post.

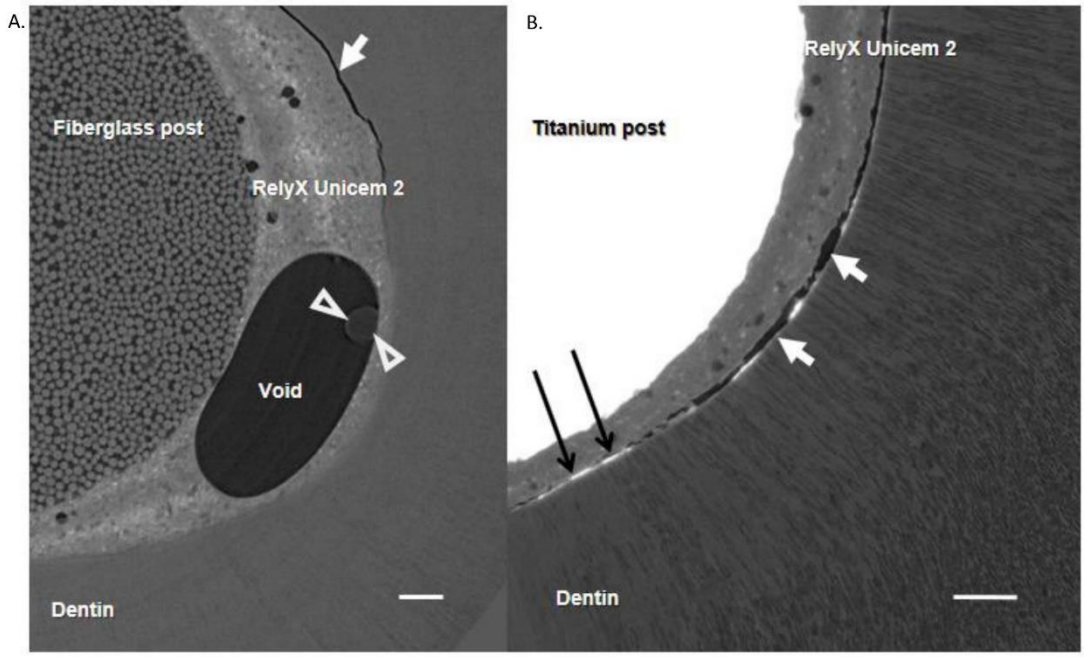

Supplementary Figure 3: High-resolution PCE-CT reveals interface features observed within 2 typical restorations: These include: traces of tubules identifiable in dentin, interfacial gaps (white arrows), zones with remnants of sealer (black arrows), air bubbles in the cement layer and a water droplet (white arrowheads) residing inside a large air bubble. Scale bar 100 µm.

4. Supporting graphs

The ratio between cement area and canal area were plotted by depth. The trend in the data exhibit the expected conicity of the canal (Supplementary Fig. 5). The correlation between canal perimeter and interfacial gaps is graphically depicted in Supplementary Fig. 6.

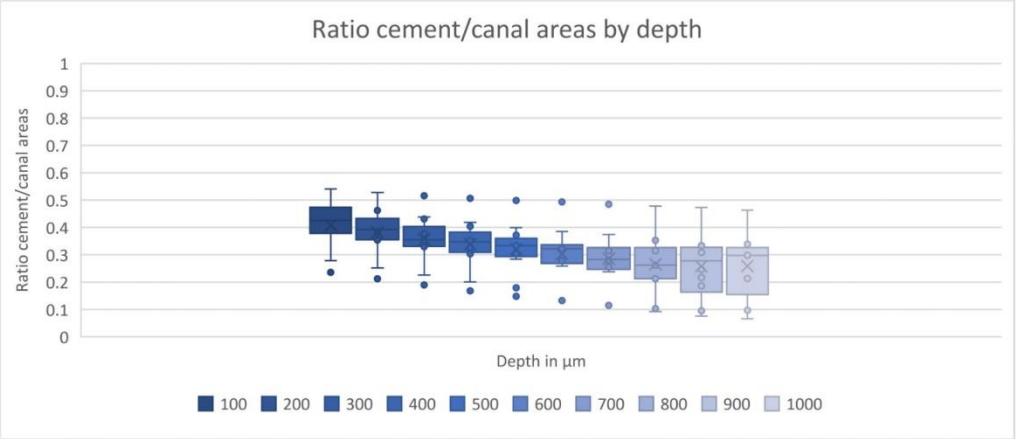

Supplementary Figure 4: boxplot of the ratios between cement area and canal area along the samples (depth in µm), showcasing a decrease in the cement filled area along the canal depth.

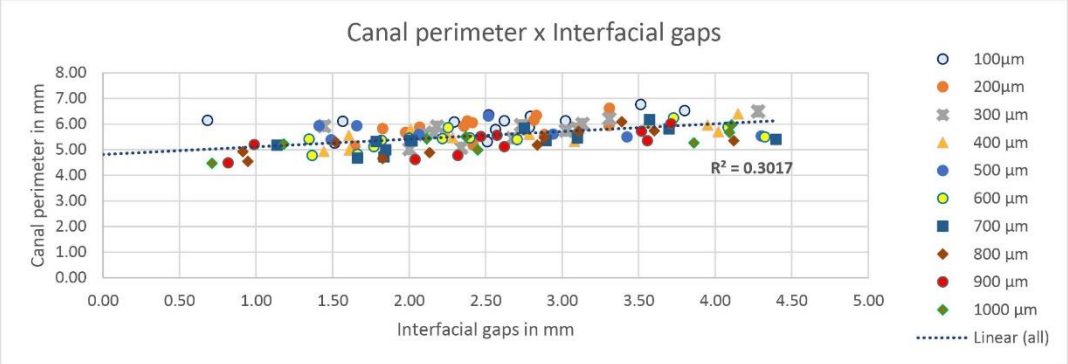

Supplementary Figure 5: plot of the canal perimeter (mm) versus the interfacial gaps length of the canal (mm), showing a moderately positive correlation (r 0.5493, p< 0.01) between both measurements.

5. Supporting table

All collected data was tabulated as shown in Supplementary table 1

Depth in µm	Canal Perimeter in mm (A)	Canal area in mm^2 (B)	Post perimeter in mm	Post area in mm^2	Cement layer area in mm^2 (C)	Gap perimeter in mm (A, B, C, D)	Sealer covered perimeter in mm (D)
			Titanium				
100	5.79 (±0.41)	2.54 (±0.30)	4.61 (±0.10)	1.61 (±0.03)	0.92 (±0.03)	1.98 (±0.87)	0.68 (±0.32)
200	5.63 (±0.39)	2.40 (± 0.26)	4.59 (±0.08)	1.59 (±0.03)	0.80 (±0.26)	2.42 (±0.62)	1.05 (±0.93)
300	5.51 (±0.40)	2.30 (± 0.25)	4.56 (±0.11)	1.57 (±0.03)	0.72 (±0.25)	2.57 (±0.48)	0.88 (±0.58)
400	5.41 (±0.40)	2.22 (± 0.25)	4.53 (±0.06)	1.56 (±0.03)	0.65 (±0.24)	2.62 (±1.21)	0.77 (±0.95)
500	5.34 (±0.42)	2.14 (± 0.26)	4.51 (±0.07)	1.54 (±0.04)	0.59 (±0.24)	2.61 (±1.15)	0.99 (±0.60)
600	5.25 (±0.42)	2.07 (± 0.26)	4.48 (±0.06)	1.53 (±0.03)	0.53 (±0.24)	2.50 (±1.33)	0.75 (±0.67)
700	5.16 (±0.44)	2.00 (± 0.26)	4.45 (±0.07)	1.51 (±0.03)	0.48 (±0.25)	2.54 (±1.19)	0.66 (±0.54)
800	5.08 (±0.46)	1.94 (± 0.27)	4.42 (±0.05)	1.50 (±0.04)	0.43 (±0.25)	2.36 (±1.24)	0.56 (±0.51)
900	5.03 (±0.48)	1.89 (± 0.27)	4.40 (±0.06)	1.48 (±0.03)	0.40 (±0.25)	2.21 (±1.18)	0.66 (±0.62)
1000	5.16 (±0.50)	1.88 (± 0.29)	4.43 (±0.05)	1.47 (±0.60)	0.40 (±0.29)	2.46 (±1.87)	0.94 (±1.21)
			Fiberglass				
100	6.27 (±0.30)	4.66 (±0.09)	4.66 (±0.09)	1.62 (±0.04)	1.39 (±0.31)	2.90 (±0.55)	0.22 (±0.24)
200	6.10 (±0.32)	4.67 (±0.11)	4.67 (±0.11)	1.60 (±0.04)	1.24 (±0.30)	2.53 (±0.47)	0.23 (±0.23)
300	5.98 (±0.30)	4.66 (±0.11)	4.66 (±0.11)	1.59 (±0.04)	1.11 (±0.30)	2.73 (±0.93)	0.32 (±0.39)
400	5.82 (±0.32)	4.64 (±0.13)	4.64 (±0.13)	1.57 (±0.04)	1.01 (±0.30)	2.83 (±0.77)	0.38 (±0.39)
500	5.70 (±0.32)	4.63 (±0.06)	4.63 (±0.06)	1.55 (±0.04)	0.93 (±0.30)	2.49 (±0.79)	0.40 (±0.26)
600	5.61 (±0.32)	4.57 (±0.09)	4.57 (±0.09)	1.54 (±0.04)	0.86 (±0.30)	2.38 (±0.73)	0.49 (±0.35)
700	5.54 (±0.35)	4.53 (±0.08)	4.53 (±0.08)	1.52 (±0.04)	0.81 (±0.30)	2.50 (±0.82)	0.61 (±0.39)
800	5.47 (±0.45)	4.50 (±0.08)	4.50 (±0.08)	1.50 (±0.04)	0.78 (±0.37)	2.63 (±0.98)	0.61 (±0.54)
900	5.56 (±0.37)	4.52 (±0.06)	4.52 (±0.06)	1.49 (±0.04)	0.83 (±0.48)	2.84 (±0.58)	0.67 (±0.28)
1000	5.48 (±0.40)	4.45 (±0.07)	4.45 (±0.07)	1.47 (±0.04)	0.78 (±0.36)	2.76 (±0.91)	0.64 (±0.33)

(A) Pearson correlation test r= 0.5493, p < 0.0001

(B) Pearson correlation test r= 0.5189, p < 0.0001

(C) Pearson correlation test r= 0.5335, p < 0.0001

(D) Pearson correlation test r= 0.5524, p < 0.0001

Supplementary table 1: Means and Standard Deviations of each measured parameter for both groups (titanium and fiberglass posts) are tabulated by depth (every 100 µm). There was no statistically significant difference between the groups (Mann Whiney, p>0.01), and there was correlation between gap perimeter (mm) and different parameters indicated by the letters: A, B, C and D.

6. References:

1. Cloetens P, Pateyron-Salomé M, Buffière JY, Peix G, Baruchel J, Peyrin F, et al. (1997) Observation of microstructure and damage in materials by phase sensitive radiography and tomography. *Journal of Applied Physics* **81**, 5878-86.
2. Moinzadeh AT, Farack L, Wilde F, Shemesh H, Zaslansky P (2016) Synchrotron-based Phase Contrast-enhanced Micro-Computed Tomography Reveals Delaminations and Material Tearing in Water-expandable Root Fillings Ex Vivo. *Journal of endodontics* **42**, 776-81.
3. Shemesh H, Lindtner T, Portoles CA, Zaslansky P. (2018) Dehydration Induces Cracking in Root Dentin Irrespective of Instrumentation: A Two-dimensional and Three-dimensional Study. *Journal of endodontics* **44**,120-5.
4. Zaslansky P, Fratzl P, Rack A, Wu MK, Wesselink PR, Shemesh H (2011) Identification of root filling interfaces by microscopy and tomography methods. *International endodontic journal* **44**, 395-401.

12. Journal Summary List for Paper 2

Paper 2: Prates Soares A, Blunck U, Bitter K, Paris S, Rack A, Zaslansky P. Hard X-ray phase-contrast-enhanced micro-CT for quantifying interfaces within brittle dense root-filling-restored human teeth. *J Synchrotron Radiat*. 2020;27(Pt 4):1015-1022.

Excerpt of the InCites Journal Citation Report in Web of Science™ by Clarivate Analytics

Journal Data Filtered By: **Selected JCR Year: 2019**, as there is no list yet for 2020.
Selected Editions: SCIE, SSCI Selected Categories: '**PHYSICS, APPLIED**'
Selected Category Scheme: WoS
In total: 155 Journals

Rank	Full Journal Title	Total Cites	Journal Impact Factor	Eigenfactor Score
1	NATURE MATERIALS	99,502	38.663	0.158590
2	Nature Photonics	45,057	31.241	0.100340
3	ADVANCED MATERIALS	264,939	27.398	0.485370
4	MATERIALS SCIENCE & ENGINEERING R-REPORTS	7,964	26.625	0.005680
5	Advanced Energy Materials	67,558	25.245	0.169210
…	…	…	…	…
73	JOURNAL OF SYNCHROTRON RADIATION	6,814	2.251	0.010390
74	JOURNAL OF MATERIALS SCIENCE-MATERIALS IN ELECTRONICS	22,337	2.220	0.027780

Paper 2 (2020)

13. Paper 2

research papers

JOURNAL OF SYNCHROTRON RADIATION

ISSN 1600-5775

Hard X-ray phase-contrast-enhanced micro-CT for quantifying interfaces within brittle dense root-filling-restored human teeth

Ana Prates Soares,[a]* Uwe Blunck,[a] Kerstin Bitter,[a] Sebastian Paris,[a] Alexander Rack[b] and Paul Zaslansky[a]*

[a]Department of Operative and Preventive Dentistry, Charité Universitätsmedizin Berlin, Aßmannshauser Straße 4-6, 14197 Berlin, Germany, and [b]ESRF – The European Synchrotron, CS 40220, Grenoble Cedex 9, Grenoble 38043, France. *Correspondence e-mail: ana.prates-soares@charite.de, paul.zaslansky@charite.de

Received 15 November 2019
Accepted 21 April 2020

Edited by A. F. Craievich, University of São Paulo, Brazil

Keywords: phase contrast enhanced micro-CT; interfacial gaps; restoration flaws; dental composites; resin bonding.

Bonding of resin composite fillings, for example following root-canal treatment, is a challenge because remaining gaps grow and lead to failure. Here, phase-contrast-enhanced micro-computed tomography (PCE-CT) is used to explore methods of non-destructive quantification of the problem, so that counter-measures can be devised. Five human central incisors with damaged crowns were root-filled followed by restoration with a dental post. Thereafter, the crowns were rebuilt with a resin composite that was bonded conventionally to the tooth with a dental adhesive system (Futurabond U). Each sample was imaged by PCE-CT in a synchrotron facility (ID19, European Synchrotron Radiation Facility) with a pixel size of 650 nm. The reconstructed datasets from each sample were segmented and analysed in a semi-automated manner using *ImageJ*. PCE-CT at sub-micrometre resolution provided images with an impressive increased contrast and detail when compared with laboratory micro-computed tomography. The interface between the dental adhesive and the tooth was often strongly disrupted by the presence of large debonded gaps (on average 34% ± 15% on all surfaces). The thickness of the gaps spanned 2 µm to 16 µm. There was a large variability in the distribution of gaps within the bonding area in each sample, with some regions around the canal exhibiting up to 100% discontinuity. Although only several micrometres thick, the extensive wide gaps may serve as gateways to biofilm leakage, leading to failure of the restorations. They can also act as stress-raising 'cracks' that are likely to expand over time in response to cyclic mechanical loading as a consequence of mastication. The observations here show how PCE-CT can be used as a non-destructive quantitative tool for understanding and improving the performance of clinically used bonded dental restorations.

1. Introduction

Extensive caries (tooth decay) causes large destruction of both crowns and roots in teeth. To fix this, the dentist restores the tooth shape and function using a combination of bonded composite materials that need to tightly adhere to the substrate. Biomaterials are typically chosen for mechanical durability and for aesthetic considerations, while matching the mechanical behaviour to the remaining tooth structure. Such dental biomaterials are used to return the tooth into function for patient satisfaction, and specifically to make sure the reconstruction withstands the repeating loads of mastication for many years. In fact, a main objective of contemporary dental treatment is to establish strong and continuous bonds between the filling and the tooth substrate. Current treatment protocols advocate bonded sealing for a variety of reasons. These include increased mechanical stability of the restoration

due to an improved distribution and resistance to stresses, as well as prevention of bacterial percolation at the interface (Hayashi *et al.*, 2017).

Indeed nowadays clinicians have at their disposal a myriad of bonding systems produced by different manufacturers (Sofan *et al.*, 2017). All are able to bond composites to remaining tooth tissues. However, the resulting interactions between biomaterial and tooth structure are still not ideal (Van Meerbeek *et al.*, 2003) and often failure occurs due to discontinuities at the interface between the adhesive and tooth tissues. Such gaps are undesirable because fluids and bacteria may penetrate, impairing the longevity of the restorations (Van Meerbeek *et al.*, 2003). Discontinuities at the interfaces also act as stress-raising 'cracks' that are highly likely to expand over time in response to cyclic mechanical loading (as a consequence of mastication, see, for example, Zaslansky *et al.*, 2016). Propagation of such cracks along paths of minimal resistance, typically at the bond interface, will eventually result in dislodgement and failure of the restoration (Tay & Pashley, 2007).

The problem of tooth bonding in dentistry is not new. Much has changed since the early works of Buonocore (1955) who introduced pre-treatment of the dental substrate by use of phosphoric acid etching. Such conditioning improves the chemical and mechanical attachment (Buonocore, 1955). This approach is as valid today as it was decades ago. Consequently, there are many routinely used products known as 'etch-and-rinse' dental bonding systems, for which phosphoric acid etching and water rinsing is required prior to application of the adhesive. Alternative products have since emerged known as 'self-etching' systems that contain acidic monomers in their composition. Such 'self-etching' products can condition the tooth while forming a chemical bond (Van Meerbeek *et al.*, 2003). More recently, so-called 'universal adhesives' have appeared on the dental-materials market, and they can be applied in both 'etch-and-rinse' and 'self-etching' modes (Sofan *et al.*, 2017). Regardless of the bonding system used, the resulting interfaces with the tooth substrate are variable in quality and remain an active field of research, often due to uncontrollable voids and gaps within the bonded region.

Of the various types of dental treatments requiring bonding, the restoration of teeth and roots largely infected and destroyed by decay is the most complex. During treatment, the root canal system needs to be disinfected prior to tooth reconstruction. Disinfection followed by sealing of the tooth root are designed to stop and prevent re-infection, and the treatment is known as 'root canal treatment'. Once the filling is completed, reconstruction of lost tooth structure must be planned. This usually requires a post-and-core restoration followed by crown construction. The post is used as a central pillar, and it is cemented into the root canal to support a composite material that replaces the bulk (core) of the crown (see example in Fig. 1). This is needed so that the post-and-core best retain a new artificial crown that is to be cemented permanently. In turn, the crown restoration provides the aesthetics and mechanical structure needed for efficient mastication. Finding materials that efficiently bond to the tooth may thus be considered essential for the long-term outcome of such restorations (Rasimick *et al.*, 2010).

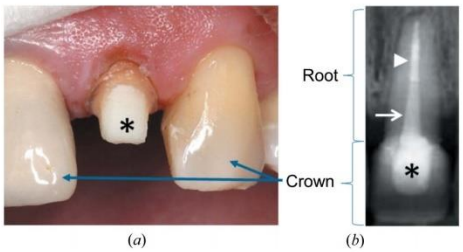

Figure 1
(*a*) Intra-oral photograph showing a tooth with a core (*), which is the only visible part of the post-and-core restoration during treatment, prior to coverage with a crown. (*b*) Radiograph of a similar tooth in which the core (*) is seen beneath an artificial crown, supported by a fibreglass post (white arrow) that is cemented into the disinfected and sealed (white arrowhead) root canal. (Clinical photographs courtesy of Drs Nestor Tzimpoulas and Wesley Thé, The Netherlands.)

For all the currently available materials on the market, establishing a continuous attachment between adhesive and tooth substrate is an ongoing challenge. It is thus important to be able to quantify the morphology and continuity of the bonded interfaces in the restored tooth, non-destructively. Indeed the quality of the bond produced depends on many factors ranging from the characteristics of the tooth surface (degree of mineralization, porosity, organic composition, *etc.*) to attributes of the bonding system (viscosity, wettability, acidity, *etc.*) (Perdigao, 2010; Cardoso *et al.*, 2011). Specifically, discontinuities at the interface known as 'interfacial gaps' are a major concern. Such gaps are usually studied by serial sectioning of the samples and microscopy imaging (Heintze, 2013), either with or without dye infiltration; dye is used to enhance the contrast of the gaps (*e.g.* organic colourants or silver nitrate) (Neves *et al.*, 2014). Overall, destructive methods such as slicing produce unwanted artefacts (Zaslansky *et al.*, 2011) whereas deep tracer infiltration may lead to 'false-positive' findings (Kriznar *et al.*, 2019; Shemesh *et al.*, 2008). Although 3D imaging techniques based on tomography are frequently used (*e.g.* Carrera *et al.*, 2015; Bakhsh *et al.*, 2011; Kwon & Park, 2012), the low density of polymer-based adhesive systems restricts the visibility of interfacial gaps using conventional X-ray imaging methods and hence it has been almost impossible to study the integrity of composite bonding (Bakhsh *et al.*, 2011).

Phase-contrast-enhanced micro-computed tomography (PCE-CT) accentuates interfaces due to the combined effects of high flux 'partial-coherence' X-rays. This facilitates the differentiation between materials with similar density (Cloetens *et al.*, 1996), in 3D, requiring no additives (*e.g.* dye) to increase contrast. 3D measurements of whole, root-treated teeth have previously been demonstrated using PCE-CT, revealing different density dental materials at micrometre resolution (Zaslansky *et al.*, 2011; Moinzadeh *et al.*, 2016; Soares *et al.*, 2019); however, application of these methods to

Table 1
Materials and descriptions of their use.

Materials and chemicals used for sample preparation are in the order of appearance in the text.

Description	Nomenclature	Manufacturer
Storage antiseptic solution	0.5% chloramine T	Merck KGaA, Darmstadt, Germany
Canal instrumentation files	Endodontic nickel titanium files	X1-X4 Pro Taper Next System, Dentsply Sirona, Ballaigues, Switzerland
Root canal disinfection solution	1% sodium hypochlorite solution	Hedinger GmbH, Stuttgart, Germany
Root canal rinsing solution	Saline solution	Braun, Melsungen, Germany
Root canal drying material	Sterilized paper filter cones	Pro Taper Next System X4 Paper Points Dentsply Sirona
Root canal sealing cone	Gutta percha	Pro Taper Next System X4 gutta percha cone, Dentsply Sirona
Root canal sealing cement	Dual paste epoxy based sealing cement	AH Plus, Dentsply Sirona
Vertical compaction of canal seal	Root canal obturation unit	Calamus Dual System, Dentsply Sirona
Dental post	Fibreglass post	Dentin Post size 090, Komet, Lemgo, Germany
Resin cement	Dual curing, self-adhesive resin cement	RelyX Unicem 2, Automix delivery system, 3M ESPE Dental Products, St Paul, USA
Acid etch	Phosphoric acid at 37%	Orbi Flow, Orbis Dental, Münster, Germany
Dental adhesive system	Universal dual-curing adhesive system	Futurabond U Single Dose, Voco, Cuxhaven, Germany (LOT No. 1601051)
Light cure	LED light curing device	Valo Corded, Ultradent Products Inc, South Jordan, USA
Resin composite	Core build up dual curing resin composite	Rebilda DC, Voco

help tackle bonded restoration is still missing. The aim of the present work is to outline a 3D quantitative approach to measure low-density inclusions at interfaces between tooth tissues and polymer-based dental adhesives, using PCE-CT in wet restored teeth.

2. Materials and methods

2.1. Sample preparation

For imaging the interfaces in restored teeth, samples were prepared using standardized clinically relevant protocols. These mimic the same working conditions followed in routine dental office procedures, as described below. For simplicity, all materials and chemicals used are listed in Table 1.

2.2. Root canal treatment

Five human upper central incisors were obtained with written informed consent under an ethics-approved protocol (EA4/102/14) by the Ethical Review Committee of the Charité Universitätsmedizin Berlin, Germany, and were stored in an antiseptic solution prior to the experiment. Each tooth had its root canal treated following a standardized protocol (Soares *et al.*, 2019) by canal instrumentation and use of disinfecting irrigation followed by canal rinsing and drying. Each root canal was sealed with a standard root filling material. The filling comprised a gutta percha cone coated with a sealing cement which was vertically compacted into the canal.

2.3. Post cementation

Following 24 h of sample storage (to allow the materials to set in a moist environment and at room temperature) each tooth was restored using a fibreglass dental post. This was cemented into the root canal with a self-adhesive resin cement, following manufacturers recommendations [for details, see Table 1 as well as Soares *et al.* (2019)]. Such dental posts are routinely used as pillars for the reconstruction of the tooth crown.

2.4. Crown restoration

Each tooth crown was restored immediately after post cementation. For that, the exposed tooth cervical area was acid etched for 10 s, followed by rinsing and air drying. A dental adhesive system was applied following manufacturers recommendations, including light curing for 10 s (Table 1, Fig. 2). A standard resin composite was placed over the adhesive layer and onto the dental post to rebuild the crown form. Following chemical polymerization (curing), the crown

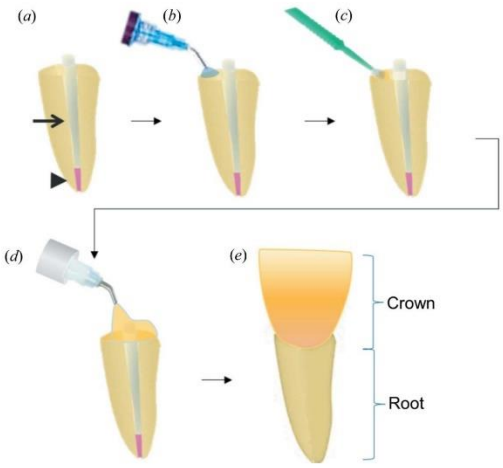

Figure 2
Typical workflow for root canal and crown restoration: (*a*) specimens after root canal treatment (seal – black arrowhead) and post (black arrow) cementation (*b*) receive acid-etching treatment of the restoration margins. The surface is then washed and briefly dried. (*c*) A universal dental adhesive (bonding system) is applied using dental brushes and light cured (photo-polymerized). (*d*) A dental resin composite is then placed on the post and on the exposed areas of the tooth to rebuild (*e*) the original crown shape.

composite was light cured for 40 s to ensure full chemical activation and cross-linking. After 5 min, the resin was sufficiently hard and the material was trimmed and polished to reach the final shape of the crown.

2.5. Imaging and reconstruction

After tooth restoration, each sample was mounted in a transparent vial (Micro tube 2 ml, Sarstedt, Nümbrecht, Germany), padded with wet foam to maintain humidity and to avoid dehydration during imaging.

Laboratory micro-computed tomography (μCT) (Skyscan 1172; Bruker micro CT, Kontich, Belgium) was used to first image each specimen (16 μm pixel size, 700 ms exposure time). Following reconstruction (NRecon 1.7.1.0; Bruker micro CT, Kontich, Belgium) the architectures of the restorations were examined in both 2D and 3D (*ImageJ* 1.52d, National Institute of Health, USA; Amira ZIB-Edition, Konrad-Zuse-Zentrum für Informationstechnik Berlin, Germany). The cervical areas, including the rim between root and the crown restoration were selected for imaging by PCE-CT in a synchrotron. Each sample was scanned on beamline ID19 of the European Synchrotron Radiation Facility (ESRF, Grenoble, France) using inline propagation-based contrast microtomography (Fig. 3). An X-ray photon energy of 34 keV was used with a pco.edge camera (PCO AG, Kelheim, Germany), and an LSO:Tb scintillator in a custom-made imaging system (OptiquePeter, Lentilly, France) with an effective pixel size of 650 nm. To enhance the visibility of gaps, PCE-CT scans were obtained using a sample-to-detector distance of 33 mm. Each sample was mounted on the high-resolution rotation stage and a total of 4900 radiographic projections were recorded (200 ms exposure times) while continuously rotating the samples by 360°. To accommodate the larger field of view, we used a horizontal stitching mode to fully image samples that were wider than a single frame of the camera. ESRF in-house code was used to reconstruct the data, enhancing contrast in the radiographs by means of a modified Paganin-based filtering (δ/β ratio of 200; Mirone *et al.*, 2014).

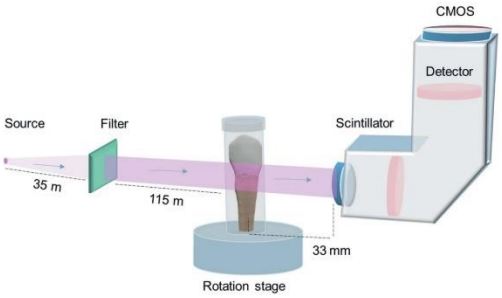

Figure 3
Schematic illustration of the experiment showing the incoming X-ray beam (source is far to the left, not drawn to scale) passing through relevant filters to reach the sample mounted on the rotation stage. The samples were kept humid in a sealed plastic vial throughout the experiment. Fresnel propagation was induced by increasing the distance between the sample and detector (33 mm) leading to edge enhancement with sufficient contrast to view the adhesive layer (Cloetens *et al.*, 1996).

2.6. Image analysis

The high-resolution reconstructed datasets characteristically contained about 2100 slices orthogonal to the long axis of the tooth. Each dataset occupies 80 Gigabytes or more of disk space. Data were visualized using *ImageJ* and *Amira*. Typical 2D slices are shown in Fig. 4 and 3D renderings of the reconstructions are shown in Figs. 5–7. Due to phase contrast enhancement at discontinuities and between different density components, details of the post, cement, voids and tooth tissues are clearly visible.

To isolate debonding and interfacial gaps, the datasets were processed using the free extension package *MorpholibJ* for *ImageJ* (Legland *et al.*, 2016). As a first step, a threshold was defined using the grey value range corresponding to gaps in the restoration [Fig. 4(*a*)]. The resulting binary images had their different sets of connected pixels and voxels individually numbered and labelled using the 'Connected components Labelling' algorithm. The different components localized to the adhesive layer were then visually selected, discarding the irrelevant (outside of the interface) labels by using the 'Select Labels' function of *MorpholibJ*. The final Boolean volume comprising only the interfacial gaps between adhesive and tooth was overlaid onto the original volume (Fig. 5) to verify successful segmentation (Fig. 6). The extracted volumes of voids were then further processed as follows: the thickness of the gaps was determined using the 'Local thickness' algorithm of *ImageJ* (Dougherty & Kunzelmann, 2007) (Fig. 7). The gap cross-sectional areas were determined by axially projecting

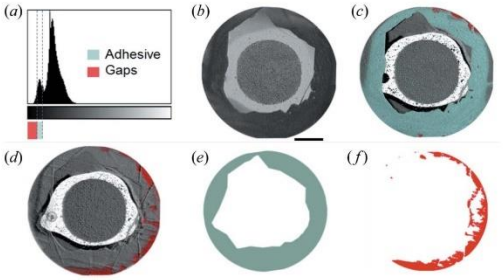

Figure 4
Proposed data processing pipeline for bonded restoration analysis of typical 3D reconstructed PCE-CT datasets: (*a*) histograms of the full volumes (*b*) were used to binarize and segment the interfacial gaps (grey value range matching the interfacial gap region is marked light blue beneath the graph abscissa). (*c*) The adhesive layer, marked light blue – compare panel (*e*) – is well defined. (*d*) Gaps at the interface (red points on the 2D slice) are also identified based on the histogram [red marked region corresponding to gaps in (*a*)]. The area of bonding between tooth and adhesive (*e*) was determined (see additional details in the text), from which the percentage of interfacial gaps (*f*) was calculated as the ratio between (*f*) and (*e*). Scale bar: 500 μm.

the minimal intensity of the segmented volume along the tooth/post axis. Similarly, the tooth area conditioned for adhesive bonding was determined by projecting the maximum intensity of the full volume, thereafter thresholding it to separate the darker (conditioned tooth area) from the brighter (cement-covered tooth area) areas. The star-like appearance, as demonstrated in Fig. 4(*b*), is due to the cutting lines, used to remove excess soft cement during restoration construction: a sharp straight scalpel was used to clear overflow prior to crown construction. Thus PCE-CT even reveals laying steps during restoration fabrication. With 2D slices containing the conditioned tooth area and gap, the percentage of gaps at the interface was calculated. Radial, orientation-specific variations in the non-bonded regions were quantified to assess the distributions of gaps at the interface. With the centre of the restoration/post defined as a pivot, the tooth and gap areas were divided in 18 equal segments (sectors) spanning 360° around the tooth long axis, each extending 20° on the tooth surface. For each sector, the ratio of gaps to the area of bonding was quantified and plotted against the azimuthal angular axis.

3. Results

Laboratory µCT scans generated datasets that reproduced the approximate geometry and the main components of the tooth restoration within the root and the reconstructed crown. In such data, however, there was no difference in contrast between the resin composites used for crown reconstruction and the resin cement (Fig. 5), nor was it possible to distinguish the adhesive polymer layer or any gaps therein. Furthermore, the interfaces between restorative materials and tooth substrate were blurred, making it impossible to evaluate the extent of bonding between the tooth tissues and the dental materials.

PCE-CT at sub-micrometre resolution provided 3D datasets with an impressive contrast and a remarkable amount of detail

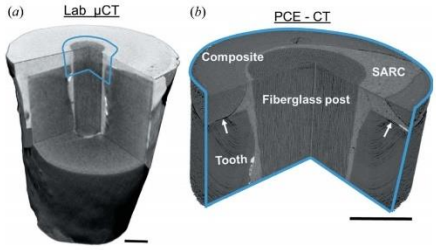

Figure 5
(*a*) Laboratory µCT images of the entire root length and a part of the crown lacking sufficient contrast to show the difference between some of the materials or to depict gaps at their interfaces. (*b*) PCE-CT revealed extensive details in the structure of the restoration, showing the morphology of the tooth and the presence of the adhesive layer (white arrows), as well as details within and the difference between the fibreglass post, self-adhesive resin cement (SARC) and the resin composite of the crown. Scale bars: 500 µm.

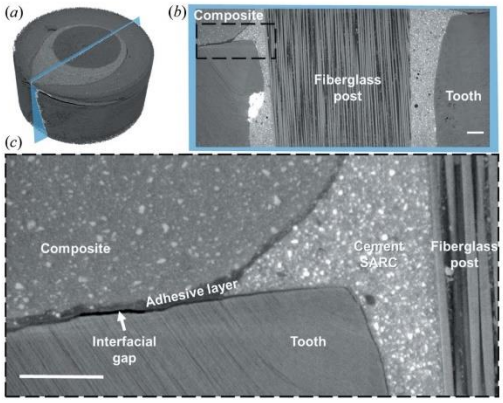

Figure 6
Full volumes (*a*) were rendered in 3D where longitudinal slices were used to verify the difference in contrast between composite, fibreglass post, SARC, tooth and adhesive layer (*b*) and (*c*). Note the presence of an interfacial gap between tooth and adhesive layer [(*c*) – white arrow] and the details appearing in the magnified inset. Scale bars: 100 µm.

(Figs. 5–7). The micromorphology of the tooth and restoration were fully visible, revealing micrometre-diameter dentin tubules, highlighting the presence of fillers in the different resin composites and well reproducing the layout of single fibres within the fibreglass post. Example overviews and slices in the datasets are shown in a longitudinal slice in Fig. 6.

The enhanced contrast brought about with PCE-CT highlights gaps between the adhesive (Fig. 6), tooth substrate and resin composite. Although significant areas of the interface appeared to be well bonded and continuous, interfacial gaps were surprisingly extensive and well identifiable. The thickness of the gaps (*e.g.* Fig. 6, white arrow) varied from 2 µm to 16 µm and adversely affected an average of 34% (±15%) of the contact surfaces between dentin and adhesive, as demonstrated here in five different teeth.

The results from the analysis of 18 sections of each sample, shown in the graphs of Fig. 7, reveal the large variability in the percentage of gaps between different sides of the same restoration in different samples. There were specimens with extreme disparities, where some segments had no gaps at the tooth-restoration interface, while others exceeded 95% of gaps. Such regions have a poor bond between the restoration and tooth tissue. The graphs highlight the variability in the total percentage of gaps between samples. Note that the interface is not a plane but is a 3D surface such that proper quantification required 3D sub-micrometre high-contrast information that is obtained non-destructively. PCE-CT provided this information, which is very different and complementary to the information from physical slicing. The latter is particularly difficult to achieve in the brittle tooth-filling interface in different directions, which may then under-represent the full extent of the problem for any given filling.

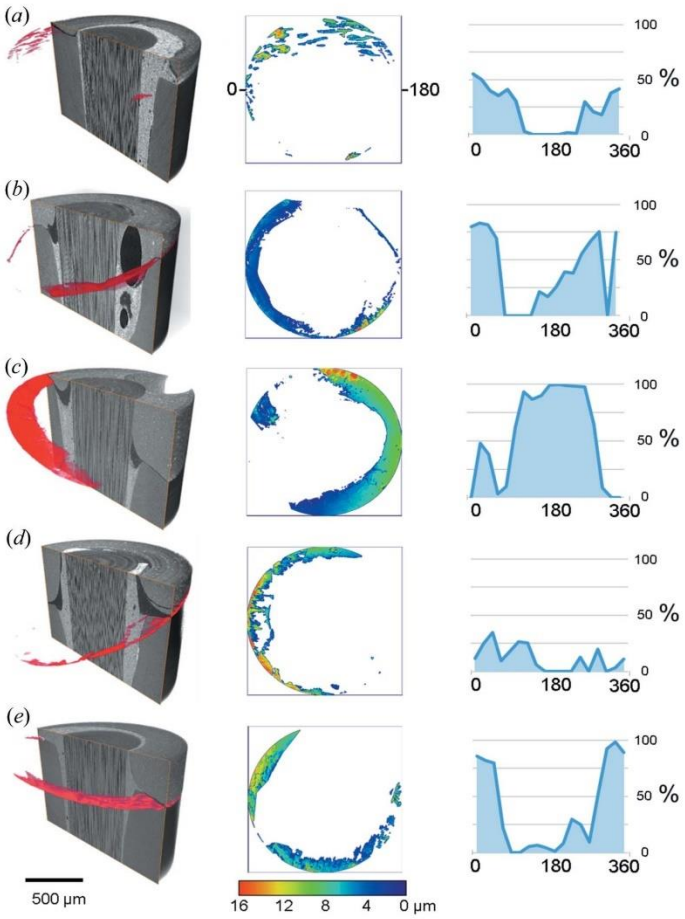

Figure 7
3D renderings of five samples (on the left), showing longitudinally sliced volumes portraying tooth and restoration materials virtually cropped (grey), on which the interfacial gaps between dentin and adhesive layer are depicted in 3D (red). Thickness maps (middle) of the interfacial gaps show a spatially varying distribution around the imaged region. The calibration bar represents the thickness of the gaps. Quantitative evaluation of the percentage of gaps measured in 18 segments around the axis of the post reveals strong orientation variation with certain regions of debonding exceeding 80% of the surface area.

4. Discussion

The present work provides a proof-of-principle feasibility test resolving the challenges involved in imaging and quantifying bonding between teeth and restorations. This has great significance for developing and validating the achievement of reliable, gap-free bonded margins. With PCE-CT it is possible to quantify and compare thin gaps (<20 µm-thick) at the interfaces in adhesively restored human teeth. Of great concern is the observation that in each tooth at least 50% of the visible section of the outer imaged rim exhibited some form of gap, as seen in the central column of Fig. 7. Achieving a complete, continuous gap-free bond in real restored teeth thus remains a challenge. The samples treated here used a material belonging to the latest generation of adhesives (Futurabond U) where ~35% of the bonded tooth surfaces exhibited discontinuous interfacial gaps. The distribution of gaps (both extent and orientation) was highly variable both within and between samples, which is typical for biomedical samples. This is an additional reason why non-destructive testing is needed for quantification and finding solutions to polymer bonding. Despite following strict protocols and treating the tested teeth under ideal, identical conditions *in vitro*, it is extremely difficult to produce a predictable sealed bonded interface. From a biological standpoint, establishing a continuous interface between tooth and adhesive is a major objective of treatment. It is a clinical objective aimed at preventing damages associated with water sorption, infiltration of bacteria and bacterial by-products, reportedly associated with secondary caries and/or re-infection of the root canal system (Van Meerbeek *et al.*, 2003). From a biomechanical standpoint, structural gaps act as stress-raisers with the result that any bending that pulls against the bonded interface results in high stress concentration. This leads to propagation of the debonded region (adhesive failure) or to propagation of cracks into the materials forming the bond (cohesive failure) (Tay & Pashley, 2007; Chen *et al.*, 2015). This is of particular concern for bonded surfaces following root canal treatment, since mechanical fatigue is very likely to occur due to structural defects beneath the restored crown used for mastication. Indeed cyclic loading is typical for teeth and restorations that must function for many years. In the long term, debonding and expansion of interfacial gaps may lead to complete detachment and failure of the tooth/restoration.

Due to the lack of contrast and resolution in the laboratory µCT images, it was not possible to observe the adhesive layer or the interfaces between materials. PCE-CT resolved this problem as it is extremely effective and may be the only possible means to non-destructively image interfacial gaps

between the low-density polymer material and other structures within the tooth restorations (Soares *et al.*, 2019). Visualizing discontinuities at the interfaces of a low-absorption dental adhesive with μCT is challenging (Mollica *et al.*, 2004; De Santis *et al.*, 2005; Kriznar *et al.*, 2019; Neves *et al.*, 2014; Carrera *et al.*, 2015). The lack of contrast between materials, unavailability of sufficient resolution and the accumulation of artefacts inherent to synchrotron-based imaging complicates the process of quantifying interfacial gaps in 3D (Kriznar *et al.*, 2019; Neves *et al.*, 2014). Previous work attempted to enhance contrast by increasing the absorption of restorative materials, adding radiopaque fillers to their composition (Rominu *et al.*, 2014). Other authors limited the use of PCE-CT to image high-absorption adhesives (rich in radiopaque particles), while applying thick layers of adhesive to the samples (Kriznar *et al.*, 2019). The adhesive used in our study has no fillers and was applied in one single layer, as recommended by the manufacturer for clinical use. Moreover, as can be seen in Fig. 6, crisp images with high signal-to-noise ratios were acquired from intact, hydrated tooth samples that were root canal treated and restored. All these make the use of PCE-CT of great interest to communities interested in improving polymer-based bonding.

Discontinuities at the interface between restorative materials and tooth substrate have been reported using high-contrast dyes such as silver nitrate. This radiopaque liquid has been widely used in dental research due to its high contrast in radiographs (Mollica *et al.*, 2004; De Santis *et al.*, 2005; Kriznar *et al.*, 2019; Neves *et al.*, 2014; Carrera *et al.*, 2015). However, it is unclear which and what dimensions of gaps are sufficiently accessible to allow penetration and visualization of the dye. Indeed, infiltration of silver nitrate into gaps in tooth specimens was shown to be suboptimal, resulting in either the underestimation or overestimation of the sizes of interfacial gaps (addressed by Kriznar *et al.*, 2019). Overestimation may occur when silver nitrate accumulates in the naturally porous morphology of the tooth. The use of PCE-CT eliminates the need to enhance contrast using any dye with the result that the location, thickness, extension and even volume of interfacial gaps can be more accurately assessed.

The use of semi-automated image segmentation presented here will benefit from further improvements but already has many advantages. Since the data are obtained non-destructively, effects of artefacts and filtering can be tested and the 3D data can be quantified in a repeatable, quantitative operator-independent way (Carrera *et al.*, 2015). This provides information at a higher dimension that better represents the spatial arrangement of materials as compared with examining 2D physical sections. The methodology described here demonstrates the importance and feasibility of analysing intact, hydrated, as-prepared human-tooth samples in 3D, circumventing the need for cutting the tooth for direct visualization. Traditional approaches to investigate interfacial gaps require sample cross-sectioning and microscopic measurements. Although informative, such approaches are destructive, and may inadvertently cause the underestimation of gaps due to accumulation of tooth tissue (smear layer) brought about by sample polishing or overestimation of gaps as a consequence of sample dehydration (Zaslansky *et al.*, 2011). Cutting and dehydration of samples for microscopic assessment, especially with scanning electron microscopes, can also lead to cracks and overestimation of gaps near the interface, due to the brittleness of the samples (Soares *et al.*, 2019). Furthermore, as shown with the examination of 18 segments around each tooth, there can be great variability in the percentage of debonding within any single sample. This observation would translate into contrasting statistics of the data if the samples were simply sliced in different directions and examined in 2D. PCE-CT, especially at energies above 30 keV, resolves all this if sufficient access to beamlines is made available. This is augmented by the fact that the samples can be imaged under humid conditions – avoiding dehydration-induced cracking (Shemesh *et al.*, 2018), hence resembling oral conditions.

Synchrotron μCT imaging is an effective tool for examining different biological samples. The high photon flux density and almost parallel beams with a wide range of energies is suited for imaging both low- and high-density structures. Phase-contrast imaging (Cloetens *et al.*, 1996) is about three orders of magnitude more sensitive to density differences than attenuation-based methods (Lewis, 2004). Additionally, the acquisition time for tomographic imaging with similar resolution to other techniques is 10 to 100 times faster (Betz *et al.*, 2007). This enables researchers to swiftly image a large range of biomaterials inside the tooth structure (Mollica *et al.*, 2004; De Santis *et al.*, 2005; Zaslansky *et al.*, 2011; Rominu *et al.*, 2014; Hedayat *et al.*, 2016; Fatima *et al.*, 2016; Moinzadeh *et al.*, 2016; Kriznar *et al.*, 2019). Although in the experiments reported here the field of view was restricted to the centre of the specimen, additional overlapping imaging or future developments in next generation facilities will make it possible to image entire tooth crowns faster and at even higher resolutions. This will provide more information about different interactions between material and substrate. Faster acquisition rates amounting to terabytes of reconstructed data will require further developments of data storage, processing and analysis. The large number of virtual slices generated for each dataset from synchrotron μCT makes manual (slice-by-slice) segmentation impractical (Meneses *et al.*, 2011). The present work showcases one tested and tried approach to analyse full volumes containing interfacial gaps in restored human teeth. Although fairly simple, it is time consuming and requires extensive computation. It is also not applicable for the clinical setting. Future developments in the field of artificial intelligence and machine learning will hopefully improve image segmentation automation (Dimiduk *et al.*, 2018; Beliaev *et al.*, 2020).

The adhesive used for testing here was Futurabond U, a clinically used universal adhesive system. It can be deployed either with or without prior acid etching of the tooth substrate (Sofan *et al.*, 2017). In the current work, phosphoric acid was used to etch the tooth substrate (dentin) before adhesive application, since the literature shows that it results in a higher bond strength between material and tooth (Cengiz & Ünal, 2019). Futurabond U has a clinically favourable *in vitro*

performance record, comparable with other universal adhesive systems (Chen *et al.*, 2015) and is thus excellent for clinical use, like many other similar products. The investigation of gaps at the interface of different adhesives may add to the data needed to improve the performance and connection between materials and substrate. Furthermore, future developments may make it possible to correlate between observations of interfacial gaps and the important effects of bond strength (Brito-Junior *et al.*, 2015; Irie *et al.*, 2010). Greater availability of PCE-CT will pave the way to assess a large number of samples that can be mechanically loaded and imaged again, to observe debonding dynamics. Such studies can broaden understanding and enable testing of novel approaches to improve interactions between adhesives and the dental substrate.

5. Conclusions

The present work provides details about steps needed to measure gaps and the areas that they affect, without the use of any tracer dye and while strictly adhering to clinically used materials and procedures allowing reproducibility and comparability. The observations here clearly establish the use of PCE-CT for advancing our understanding about the ability of clinically used dental adhesive systems to form continuous interfaces with tooth tissues when measured *in vitro*. It is also a valuable tool for imaging interfacial gaps between thin polymer adhesives and tooth substrate in restored hydrated, treated teeth in 3D. Flaws in the thin polymer bonding layer were quantified non-destructively. Although a possible quantitative data processing pipeline was proposed, much more can be done for improved image segmentation and analysis. The use of PCE-CT will assist efforts to systematically assess the integrity of contact between different clinically used dental materials.

Acknowledgements

We thank Dr Nestor Tzimpoulas and Dr Wesley Thé for providing the clinical photographs in this publication; the European Synchrotron Radiation Facility for imaging beam time on ID19; and the Zuse Institute Berlin (ZIB) for providing access and use to a non-commercial version of *Amira* (ZIB edition) for 3D data/image visualization.

Funding information

The following funding is acknowledged: Elsa Neumann scholarship Stipendium des Landes Berlin.

References

Bakhsh, T. A., Sadr, A., Shimada, Y., Tagami, J. & Sumi, Y. (2011). *Dent. Mater.* **27**, 915–925.
Beliaev, M., Zöllner, D., Pacureanu, A., Zaslansky, P., Bertinetti, L. & Zlotnikov, I. (2020). *J. Struct. Biol.* **209**, 107432.
Betz, O., Wegst, U., Weide, D., Heethoff, M., Helfen, L., Lee, W. & Cloetens, P. (2007). *J. Microsc.* **227**, 51–71.
Brito-Junior, M., Leoni, G. B., Pereira, R. D., Faria-e-Silva, A. L., Gomes, E. A., Silva-Sousa, Y. T. & Sousa-Neto, M. D. (2015). *J. Endod.* **41**, 2058–2063.
Buonocore, M. G. (1955). *J. Dent. Res.* **34**, 849–853.
Cardoso, M. V., de Almeida Neves, A., Mine, A., Coutinho, E., Van Landuyt, K., De Munck, J. & Van Meerbeek, B. (2011). *Aust. Dent. J.* **56**, 31–44.
Carrera, C. A., Lan, C., Escobar-Sanabria, D., Li, Y., Rudney, J., Aparicio, C. & Fok, A. (2015). *Dent. Mater.* **31**, 382–390.
Cengiz, T. & Ünal, M. (2019). *Microsc. Res. Tech.* **82**, 1032–1040.
Chen, C., Niu, L. N., Xie, H., Zhang, Z. Y., Zhou, L. Q., Jiao, K., Chen, J. H., Pashley, D. H. & Tay, F. R. (2015). *J. Dent.* **43**, 525–536.
Cloetens, P., Barrett, R., Baruchel, J., Guigay, J.-P. & Schlenker, M. (1996). *J. Phys. D Appl. Phys.* **29**, 133–146.
De Santis, R., Mollica, F., Prisco, D., Rengo, S., Ambrosio, L. & Nicolais, L. (2005). *Biomaterials*, **26**, 257–270.
Dimiduk, D. M., Holm, E. A. & Niezgoda, S. R. (2018). *Integr. Mater. Manuf. Innov.* **7**, 157–172.
Dougherty, R. P. & Kunzelmann, K. H. (2007). *Microsc. Microanal.* **13**, 1678–1679.
Fatima, A., Kulkarni, V. K., Banda, N. R., Agrawal, A. K., Singh, B., Sarkar, P. S., Tripathi, S., Shripathi, T., Kashyap, Y. & Sinha, A. (2016). *J. X-ray Sci. Technol.* **24**, 119–132.
Hayashi, J., Shimada, Y., Tagami, J., Sumi, Y. & Sadr, A. (2017). *J. Dent. Res.* **96**, 992–998.
Hedayat, A., Nagy, N., Packota, G., Monteith, J., Allen, D., Wysokinski, T. & Zhu, N. (2016). *J. Synchrotron Rad.* **23**, 777–782.
Heintze, S. D. (2013). *Dent. Mater.* **29**, 59–84.
Irie, M., Maruo, Y., Nishigawa, G., Suzuki, K. & Watts, D. C. (2010). *Dent. Mater.* **26**, 608–615.
Kriznar, I., Zanini, F. & Fidler, A. (2019). *Clin. Oral Investig.* **23**, 2371–2381.
Kwon, O.-H. & Park, S.-H. (2012). *Restor. Dent. Endod.* **37**,41–49.
Legland, D., Arganda-Carreras, I. & Andrey, P. (2016). *Bioinformatics*, **32**, 3532–3534.
Lewis, R. A. (2004). *Phys. Med. Biol.* **49**, 3573.
Meneses, A. A. M., Giusti, A., Almeida, A. P., Nogueira, L. P., Braz, D., Barroso, R. C. & de Almeida, C. E. (2011). *Nucl. Instrum. Methods Phys. Res. A*, **660**, 121–129.
Mirone, A., Brun, E., Gouillart, E., Tafforeau, P. & Kieffer, J. (2014). *Nucl. Instrum. Methods Phys. Res. B*, **324**, 41–48.
Moinzadeh, A. T., Farack, L., Wilde, F., Shemesh, H. & Zaslansky, P. (2016). *J. Endod.* **42**, 776–781.
Mollica, F., De Santis, R., Ambrosio, L., Nicolais, L., Prisco, D. & Rengo, S. (2004). *J. Mater. Sci. Mater. Med.* **15**, 485–492.
Neves, A. A., Jaecques, S., Van Ende, A., Cardoso, M. V., Coutinho, E., Lührs AK Zicari, F. & Van Meerbeek, B. (2014). *Dent. Mater.* **30**, 799–807.
Perdigao, J. (2010). *Dent. Mater.* **26**, e24–e37.
Rasimick, B. J., Wan, J., Musikant, B. L. & Deutsch, A. S. (2010). *J. Prosthodont.* **19**, 639–646.
Rominu, M., Manescu, A., Sinescu, C., Negrutiu, M. L., Topala, F., Rominu, R. O., Bradu, A., Jackson, D. A., Giuliani, A. & Podoleanu, A. G. (2014). *Dent. Mater.* **30**, 417–423.
Shemesh, H., Lindtner, T., Portoles, C. A. & Zaslansky, P. (2018). *J. Endod.* **44**, 120–125.
Shemesh, H., Souza, E. M., Wu, M. K. & Wesselink, P. R. (2008). *Int. Endod. J.* **41**, 869–872.
Soares, A. P., Bitter, K., Lagrange, A., Rack, A., Shemesh, H. & Zaslansky, P. (2019). *Int. Endod. J.* **53**, 392–402.
Sofan, E., Sofan, A., Palaia, G., Tenore, G., Romeo, U. & Migliau, G. (2017). *Ann. Stomatol. (Roma)*, **8**, 1–17.
Tay, F. R. & Pashley, D. H. (2007). *J. Endod.* **33**, 391–398.
Van Meerbeek, B., De Munck, J., Yoshida, Y., Inoue, S., Vargas, M., Vijay, P., Van Landuyt, K., Lambrechts, P. & Vanherle, G. (2003). *Oper. Dent.* **28**, 1–20.
Zaslansky, P., Currey, J. D. & Fleck, C. (2016). *Bioinspir. Biomim.* **11**, 051003.
Zaslansky, P., Fratzl, P., Rack, A., Wu, M. K. & Wesselink, P. R. (2011). *Int. Endod. J.* **44**, 395–401.

14. Journal Summary List for Paper 3

Paper 3: Soares AP, Baum D, Hesse B, Kupsch A, Müller BR, Zaslansky P. Scattering and phase-contrast X-ray methods reveal damage to glass fibers in endodontic posts following dental bur trimming. *Dent Mater*. 2021 Feb;37(2):201-211.

Excerpt of the InCites Journal Citation Report in Web of Science™ by Clarivate Analytics

Journal Data Filtered By: **Selected JCR Year: 2019**, as there is no list yet for 2021.
Selected Editions: SCIE, SSCI Selected Categories: '**DENTISTRY, ORAL SURGERY & MEDICINE**'
Selected Category Scheme: WoS
In total: 91 Journals

Rank	Full Journal Title	Total Cites	Journal Impact Factor	Eigenfactor Score
1	PERIODONTOLOGY 2000	5,159	7.718	0.006380
2	JOURNAL OF CLINICAL PERIODONTOLOGY	14,785	5.241	0.013050
3	JOURNAL OF DENTAL RESEARCH	20,557	4.914	0.019900
4	DENTAL MATERIALS	15,316	4.495	0.013480
5	ORAL ONCOLOGY	10,286	3.979	0.015780
6	INTERNATIONAL ENDODONTIC JOURNAL	7,453	3.801	0.000666
7	JOURNAL OF PERIODONTOLOGY	16,306	3.742	0.010160
8	CLINICAL ORAL IMPLANTS RESEARCH	14,178	3.723	0.013970
9	Clinical Implant Dentistry and Related Research	4,496	3.396	0.008290
10	JOURNAL OF DENTISTRY	9,650	3.242	0.011330
11	Clinical Implant Dentistry and Related Research	3,633	3.097	0.008520
12	INTERNATIONAL ENDODONTIC JOURNAL	7,002	3.015	0.001650

Paper 3 (2021)

15. Paper 3

https://doi.org/10.1016/j.dental.2020.10.018

https://doi.org/10.1016/j.dental.2020.10.018

https://doi.org/10.1016/j.dental.2020.10.018

https://doi.org/10.1016/j.dental.2020.10.018

https://doi.org/10.1016/j.dental.2020.10.018

https://doi.org/10.1016/j.dental.2020.10.018

https://doi.org/10.1016/j.dental.2020.10.018

https://doi.org/10.1016/j.dental.2020.10.018

https://doi.org/10.1016/j.dental.2020.10.018

https://doi.org/10.1016/j.dental.2020.10.018

https://doi.org/10.1016/j.dental.2020.10.018

https://doi.org/10.1016/j.dental.2020.10.018

https://doi.org/10.1016/j.dental.2020.10.018

https://doi.org/10.1016/j.dental.2020.10.018

https://doi.org/10.1016/j.dental.2020.10.018

https://doi.org/10.1016/j.dental.2020.10.018

https://doi.org/10.1016/j.dental.2020.10.018

https://doi.org/10.1016/j.dental.2020.10.018

16. Curriculum Vitae

My curriculum vitae does not appear in the electronic version of my paper for reasons of data protection.

17. Complete list of publications with Impact factors (IF)

First author publications

1. **Soares, Ana Prates;** Baum D; Hesse B; et al. Scattering and phase-contrast X-ray methods reveal damage to glass fibers in endodontic posts following dental bur trimming. *Dental Materials*. (2020). https://doi.org/10.1016/j.dental.2020.10.018 (IF: 4.495)
2. **Soares, Ana Prates**; Blunck U; Bitter K; et al. Hard X-ray phase-contrast-enhanced micro-CT for quantifying interfaces within brittle dense root-filling-restored human teeth. *J. Synchrotron Rad.* (2020) 27, 1015-1022, https://doi.org/10.1107/S1600577520005603 (IF: 2.251)
3. **Soares, Ana Prates**; Bitter K; Lagrange A; et al. Gaps at the interface between dentine and self-adhesive resin cement in post-endodontic restorations quantified in 3D by phase contrast-enhanced micro-CT. *Int Endod J.* (2020) 53, 392-402. https://doi.org/10.1111/iej.13232 (IF: 4.63)
4. **Soares, Ana Prates**; Do Espírito Santo RF; Line SRP; et al. Bisphosphonates: pharmacokinetics, bioavailability, mechanisms of action, clinical applications in children, and effects on tooth development. *Environ Toxicol Pharmacol.* (2016) 42, 212-217. doi: 10.1016/j.etap.2016.01.015 (IF: 4.62)
5. **Soares, Ana Prates**; Do Espírito Santo RF; Line SRP; et al. Effects of Pamidronate on Dental Enamel Formation Assessed by Light Microscopy, Energy-Dispersive X-Ray Analysis, Scanning Electron Microscopy, and Microhardness Testing. *Microsc Microanal.* (2016) 22, 640-648. doi: 10.1017/S1431927616000726 (IF: 3.414)
6. **Soares, Ana Prates**; Knop LAH; Jesus AA; et al. Stem cells in Dentistry. *Rev Dental Press de Ortod e Ortop Facial.* (2007) 12, 33-40. https://doi.org/10.1590/S1415-54192007000100006 (IF: 0.0127)

Co-author publications

1. Sturm R; **Soares, Ana Prates**; et al. Interface analysis after fatigue loading of adhesively luted bundled fiber posts to human root canal dentin. *J Mech Behav Biomed Mater*. (2021) 119:104385. https://doi.org/ 10.1016/j.jmbbm.2021.104385 (IF: 3.372)
2. Mustafa HA; **Soares, Ana Prates**; et al. The forgotten merits of GIC restorations: a systematic review. *Clin Oral Investig.* (2020) 24, 2189-2201. https://doi.org/10.1007/s00784-020-03334-0 (IF: 3.07)
3. Ziouti F; **Soares, Ana Prates**; et al. An Early Myeloma Bone Disease Model in Skeletally Mature Mice as a Platform for Biomaterial Characterization of the Extracellular Matrix. *J Oncol.* (2020) https://doi.org/10.1155/2020/3985315 (IF: 2.206)
4. Ziv E; Milgram J; Davis J; **Soares, Ana Prates**; et al. Neither cortical nor trabecular: An unusual type of bone in the heavy-load-bearing lower pharyngeal jaw of the black drum (Pogonias cromis). *Acta Biomater.* (2020) 104, 28-38. https://doi.org/10.1016/j.actbio.2020.01.001 (IF: 7.242)
5. Bitter K; Falcon L; **Soares, Ana Prates**; et al. Effect of Application Mode on Bond Strength of Adhesively Luted Glass-fiber Bundles Inside the Root Canal. *J Adhes Dent.* (2019) 21, 517-524. doi:10.3290/j.jad.a43507 (IF: 2.379)
6. Silva BLL; Medeiros DL; **Soares, Ana Prates**, et al. Type 1 diabetes mellitus effects on dental enamel formation revealed by microscopy and microanalysis. *J Oral Pathol Med.* (2018) 47, 306-313. doi:10.1111/jop.12669 (IF: 2.495)
7. Knop LAH; **Soares, Ana Prates**; et al. Characterization of surface topography and chemical composition of mini-implants. *Braz J Oral Sci.* (2015) 14, 251-255, https://doi.org/10.1590/1677-3225v14n3a15 (IF: 0.26)
8. Jesus AA; SOARES, MBP; **Soares, Ana Prates**, et al. Harvest and culture of stem cells from human exfoliated deciduous teeth: technique and case report. *Dental Press J. Orthod.* (2011) 16, 111-118. http://dx.doi.org/10.1590/S2176-94512011000600017 (IF: 0.0256)
9. Barros SG; **Soares, Ana Prates**; et al. Distribution of dental surgeons throughout the State of Bahia territory, 2007. *Revista Baiana de Saúde Pública*. (2009) 33, 16- 27. https://doi.org/10.22278/2318-2660.2009.v33.n2.a202 (IF: No registry)
10. Medrado A; **Soares, Ana Prates**; et al. Influence of laser photobiomodulation upon connective tissue remodeling during wound healing. *J Photochem Photobiol B.* (2008) 92, 144-152. doi: 10.1016/j.jphotobiol.2008.05.008 (IF: 2.44)
11. Oliveira Junior SR, CANGUSSU MCT, LOPES LS, **Soares, Ana Prates**, et al. Dental fluorosis in schoolchildren 12 and 15 years of age in Salvador, Bahia, Brazil, in 2001 and 2004.*Cadernos de Saúde Pública (FIOCRUZ).* (2006) 22,1201-1206. http://dx.doi.org/10.1590/S0102-311X2006000600009 (IF: 0.1891)

18. Acknowledgements

I am deeply grateful for the opportunity to develop my PhD work at the Zahnklinik Charité Berlin, it has been a wonderful and challenging feat. None of this work would be possible without funding from the Elsa Neumann Stipendium des Landes Berlin and from the Abschluss Stipend of the Berlin Brandenburg School of Regenerative Therapies (BSRT).

I want to express great gratitude to my supervisor, Dr. Paul Zaslansky, for his mentorship and encouragement, his support for my research project and for the chance to work daily producing exciting cutting-edge science. I would also like to thank my first and second advisors, Dr. Sebastian Paris and Dr. Kerstin Bitter for helping me advance my research and for stimulating me to keep my perspective on the impact of my work.

I am grateful to the team at the Zahnklinik, for keeping an optimistic and organized environment, specially Daniela Heim for her assistance, efficiency and friendliness. To the colleagues in AGZaslansky, thank you for the trust, for the shared time and for the laughs.

Many of my collaborators have been generous teachers and have starkly helped me develop my skills, for that I am especially grateful to Dr. Bernhard Hesse, Dr. Daniel Baum, Dr. Hagay Shemesh and Dr. Uwe Blunk.

Furthermore, the experiments in different synchrotron facilities have importantly enriched my PhD experience. I appreciate the support given by the different beamline scientists and their teams and I am especially grateful to Dr. Alexander Rack, Dr. Bernd Müller and Dr. Andrew King.

To Dr. Sabine Bartosch and Bianca Kühn from the Berlin-Brandenburg School of Regenerative Therapies (BSRT), thank you for the opportunity to be a graduate student in such a stimulating environment.

To the friends I made along the way and have become part of my chosen family, thank you for all the joy, love and care. They were essential to keep focus and balance.

Most of all I am grateful to my family for their unconditional love and for teaching me how to be.